NANO · MICRO small
www.small-journal.com

From Water Solutions to Ionic Liquids with Solid State Nanopores as a Perspective to Study Transport and Translocation Phenomena

Sanjin Marion, Nataša Vučemilović-Alagić, Mario Špadina, Aleksandra Radenović, and Ana-Sunčana Smith**

Solid state nanopores are single-molecular devices governed by nanoscale physics with a broad potential for technological applications. However, the control of translocation speed in these systems is still limited. Ionic liquids are molten salts which are commonly used as alternate solvents enabling the regulation of the chemical and physical interactions on solid–liquid interfaces. While their combination can be challenging to the understanding of nanoscopic processes, there has been limited attempts on bringing these two together. While summarizing the state of the art and open questions in these fields, several major advances are presented with a perspective on the next steps in the investigations of ionic-liquid filled nanopores, both from a theoretical and experimental standpoint. By analogy to aqueous solutions, it is argued that ionic liquids and nanopores can be combined to provide new nanofluidic functionalities, as well as to help resolve some of the pertinent problems in understanding transport phenomena in confined ionic liquids and providing better control of the speed of translocating analytes.

1. Introduction

Solid state nanopores are label-free sensing platforms able to characterize single biomolecules and probe nanoscale physics.[1] Unlike biological pores, solid state pores allow easy control over the shape and degree of nanoconfinement.[2] From the fundamental point of view, nanopores, and the related nanochannels, enable studies of physical phenomena on the molecular scale.[3–5] Generally, when the diameter of nanopores is reduced to below tens of nanometers, they can become selective to ions[6] and can provide information on the effective diffusion constants of different ion species.[7] Nanopores can, furthermore, act as building blocks for various nanoscale devices, which have found several important technical applications. Consequently, they are used as ion pumps,[8] electrical diodes,[9] desalination membranes,[10] or osmotic power generation devices,[11] all due to their peculiar ion and fluid transport properties.

Ionic liquids (IL) are salts, which due to poorly coordinated ions, exist as liquids in a broad range of temperatures including standard conditions. As a class of Coulomb fluids (condensed matter with dispersed mobile charged particles), they are promising candidates for a whole new generation of electrochemical energy-storage devices (batteries, supercapacitors).[12,13] Further applications involve usage as solvents in chemical reactions, and in bioscience due to their electrochemical stability and adaptability potential ,[14–16] or as a next generation lubricant.[17] With over 1000 synthesized ionic liquids,[18] and about 10^{18} theoretical possibilities,[19] one could tailor the ionic liquid to the particular use in question.

A typical experimental realization of the nanopore system involves immersing a membrane in an aqueous solution and imposing a potential difference between the two sides (see **Figure 1**a and **Figure 2**a). Consequently, an analyte translocates through the pore on the membrane and its passage is recorded by measuring a change in the ionic current flowing through the pore. Through this types of measurements, the properties of the analyte such as size, shape, and charge can be determined with great accuracy in as low as atto-molar analyte concentrations,[20] Due to their sensitivity, nanopores have become the tool of choice for DNA sequencing.[21,22] Biological pores, such as alpha-hemolysin,[23] MspA,[24] Csg,[25] and many others are able to discriminate single-nucleotides from conductance changes of the whole sample allowing for commercially available DNA sequencing. Solid state nanopores are expected to surpass biological pores due to their chemical resilience, thermal stability, and potential for integration either with local (transverse) sensing electrodes[26] or with plasmonic nanostructure that can enhance and focus electromagnetic radiation to a nanoscale volume situated at the nanopore.[27]

Still, a common issue with solid-state nanopores is the speed of translocation, which can be so fast that the associated signal

Dr. S. Marion, Prof. A. Radenović
Laboratory of Nanoscale Biology
Institute of Bioengineering, School of Engineering
EPFL 1015, Lausanne, Switzerland
E-mail: aleksandra.radenovic@epfl.ch
N. Vučemilović-Alagić, Dr. M. Špadina, Prof. A.-S. Smith
Group for Computational Life Sciences
Ruđer Bošković Institute, Division of Physical Chemistry
10000, Zagreb, Croatia
N. Vučemilović-Alagić, Prof. A.-S. Smith
PULS Group, Physics Department
Interdisciplinary Center for Nanostructured Films
FAU Erlangen-Nürnberg 91058, Erlangen, Germany
E-mail: smith@physik.fau.de, asmith@irb.hr
The ORCID identification number(s) for the author(s) of this article can be found under https://doi.org/10.1002/smll.202100777.

DOI: 10.1002/smll.202100777

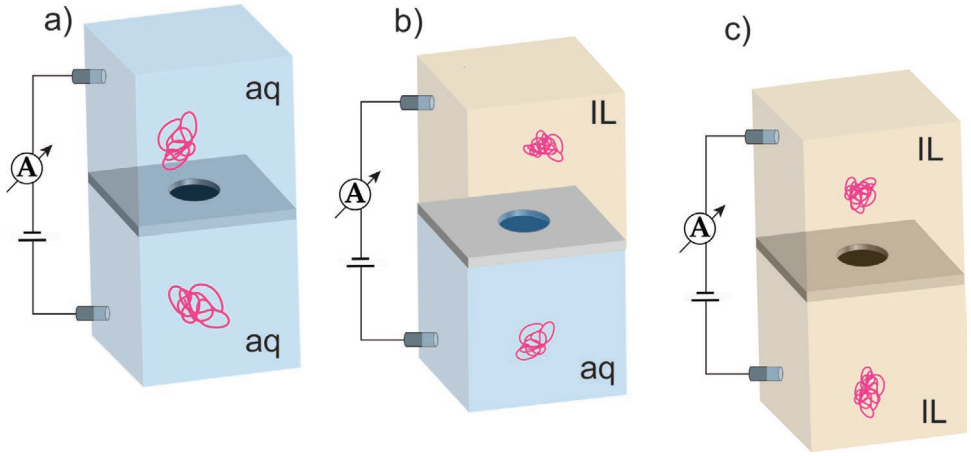

Figure 1. Types of nanopore setups discussed in this work: a) aqueous solutions in both compartments, b) ionic liquid in one, and the aqueous solution in the other compartment, c) ionic liquids at both sides of the membrane.

becomes just a single very narrow peak from which it is not possible the recognize relevant features. The two current obstacles in solid-state nanopores application for sequencing applications are better spatial resolution and slowing (control) of the translocation velocity. The translocation velocity of a free DNA molecule is orders of magnitudes faster (3000–50 000 nucleotides per ms)[21] than the optimal velocity (1–50 nucleotides per ms).[28] One approach is to use active single molecule methods to directly manipulate single DNA molecules[29–32] albeit at the cost of significantly limiting statistics. Passive methods, by modifying the properties of either the solute, solution, or nanopore surface, would have the advantage of being easily multiplexed thus providing a large dataset and ease of use. Attempts have been made using temperature variation,[33] salt concentration gradients,[34] changing the surface charge of the nanopore with light irradiation,[35] and entangling the DNA in gels during translocations,[36] etc. Aqueous solutions with multivalent electrolytes are undesirable due to Manning condensation that causes DNA to bundle.[37] On the other hand, ILs possess certain beneficial characteristics in this regard, such as structural ordering on the nanoscale and high viscosity, which have put them in the spotlight as a possible solution to tackle this issue.

First indications that complex ions such as ILs could benefit the nanopore field came from the experimental work with biological nanopores. The use of BMim-Cl solute for translocation experiments with DNA allowed a slow down of the dwell times in biological pores with pore sizes comparable to the DNA width,[38] albeit at sufficiently low concentrations it could inhibit translocations due to DNA-$[Bmim]^+$ complexation and collapse

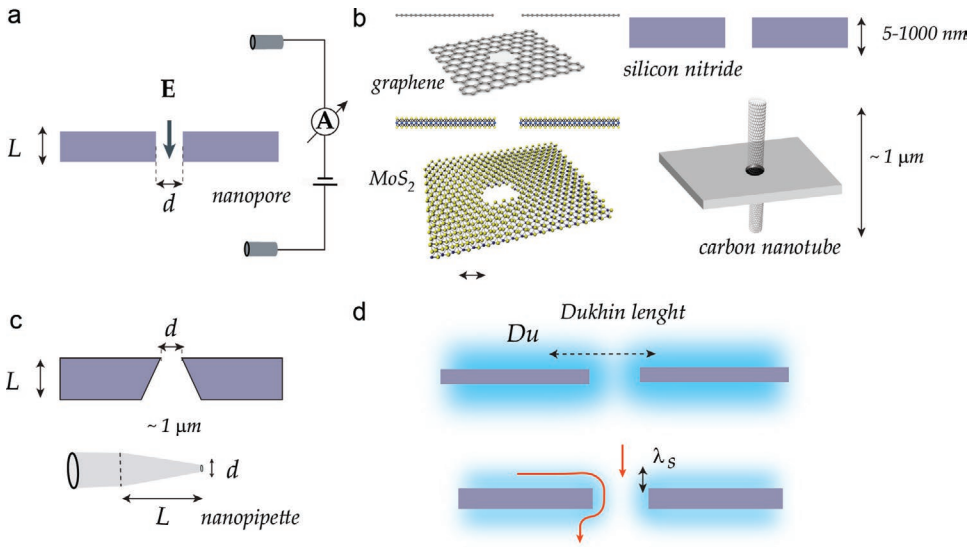

Figure 2. Typical solid state nanopore geometries. a) Schematic of a typical nanopore detection scheme, *L* marks the membrane thickness and *d* the nanopore diameter which can vary in some geometries down to nanometers. *E* marks the location and direction of the largest magnitude of the electrical field. b) Examples of typical materials used in nanopore experiments spanning from single atom thick (graphene) to hundreds of nanometers. c) Nanopores with asymmetrical (conical) geometries. d) Schematic representation of the Dukhin length overlap connected to nanopore selectivity and two major contributions to nanopore conductance via bulk and surface "pathways".

of the DNA into a globule.[39] Another application was the detection of explosive compounds in biological pores without the use of standard salts.[40] BMim-Cl in addition to being soluble in water allows Faradaic charge transfer to standard chlorinated silver (Ag/AgCl) electrodes enabling stable current recordings essential for translocation experiments. In both cases, interactions of the analyte with the pore are modulated by the presence of the ionic liquid cation. Whether this happens due to a modification of the pore surface charges as seen through the streaming potential, or through binding to the analyte, is unclear.

While these preliminary experiments can be used as a proof of principle that ILs can be used to optimize the translocation speed, they also opened a number of questions related to diffusive and driven transport through the pore, which clearly depends on the interaction of the two different solvents with the pore walls, the interface between the liquids, and the interactions of both liquids with the analyte. Apart from the aforementioned application to nucleotides sequencing, an additional benefit of nanopores is that they are at the same time an ideal tool for the study of nanoscale behavior of ILs themselves. This is in contrast to the standard experimental techniques which work with ensemble averages. So far ionic liquids have seen only limited use with solid state nanopores both in theoretical modeling[41–43] and experiments.[44–48] Notable is the recent demonstration of the dramatic slowdown of DNA translocations in 2D nanopores with an interface between an aqueous KCl salt solution and a pure ionic liquid.[46] Our aim is to provide an overview of the related theoretical and experimental research done on ionic liquids, and put a perspective on ionic liquids and other classes of Coulomb fluids[49] in expanding the versatility of solid state nanopores as both single-molecular sensors and probes of nanoscale physics. We will first briefly explain the basic physics of nanopores in simple salt solutions (non ionic liquid).

2. Nanopores as Nanofluidic Devices and Single-Molecular Tools with Simple Salts

In order to understand the advantages and disadvantages of solid state nanopores, we will introduce a simplified overview of the basic length scales and geometries involved. Nanopores, in contrast to porous materials, have a well defined, usually single, pore in the diameter range below ≈100 nm separating two chambers filled with liquids (Figure 2).[1] Electrodes measure the ion transport between these two chambers where in ideal cases the only transport pathway is through the nanopore. The electrodes are sufficiently far away from the nanopore and have a large surface area supporting Faradaic charge transfer to the two liquids so that their influence can be ignored. In this case, the nanopore is the dominant limiting factor to the current flowing through such a system. In the case that the electrode materials do not support sufficient charge transfer, the electrodes will limit the current and reliable measurements using direct current are usually impossible or at least unstable, depending on the electrode materials. Alternatively, if a suitable combination of electrodes and ionic liquids cannot be found, alternating current can be used.[48]

Different nanopore thicknesses L are possible depending on the manufacturing details (Figure 2). Nanopore thickness can vary from 2D materials with single atomic layers like graphene,[50] three atomic layers in the case of molybdenum disulphide (MoS_2),[51] or up to microns in length in the case of carbon nanotubes,[52] polymer-based track etched membranes,[53] or glass nanocapillaries.[54] Another important property is the degree of spatial asymmetry which is emphasized in the case of conical pores or glass nanocapillaries. 2D materials[55] like graphene[50] and MoS_2[51] have become a popular membrane because their thickness is comparable to the size of single nucleotides and ions allowing good spatial resolution for translocation experiments.

A simplified and rough approach we will take here would be to divide nanopores into those where the ion transport properties of the nanopore are dominated by the interplay of surface and bulk contribution, and those where the finite structure of the analyte and surface needs to be taken into account. Note that this rough but intuitive approach takes into account both the molecular nature of the corresponding fluid and the geometry and material properties of nanopores, in terms of their hydrophilicity/hydrophobicity and charging properties. Surface chemistry and physisorption should be always considered with care, and fine-tuned for the particular application.

In a classical system, dilute aqueous solutions can usually be modeled using continuum models. This transition will happen somewhere around ≈1 nm in size for a typical dilute or even less in concentrated aqueous solutions of simple salts[3,4] or when the fine (molecular) structure of the analyte starts to interact with the nanopore surface. On the other hand, ILs are expected to have a "transition" in behavior at much larger length scales, and it is unclear whether the transition is even comparable to dilute aqueous solutions of 1:1 salts, on which most continuum approaches are based. When finite size effects start to dominate, typical modeling approaches revert to using all-atom simulation methods, or mean field models that include the molecular structure of all particles in the system. This is important since solvent effect cannot be reduced to only the background dielectric response, for example, dielectric constant ε_r.[56,57] For larger nanopore widths, where bulk properties can be established inside the nanopore, there is still a clear distinction between this "mobile" (diffuse) part and stagnant (condensed) layer of ions to the surface, and one can anticipate the effect on the measured ionic conductance.[58] The ion transport in nanopores, which have diameters and thicknesses comparable to the size of small molecules, can show a wide plethora of complex phenomena and can even be used to probe individual ion size and solvation.[59] Experimentally, the probing of finite size ion effects is just within the reach of current experimental capabilities.

Most advanced ion transport functionalities seen so far in nanopores with simple ions, like ion selectivity[6] and ionic current rectification,[60] are a direct consequence of the surface charges present on the nanopore walls and how it influences the charge distributions in the bulk regions at the pore. Ion selectivity arises when a nanopore preferentially allows the passage of a subgroup of ions, and is strongest when the nanopore diameter is comparable to the electrostatic screening length which is equal to the Debye length l_D for dilute solutions

(Figure 2d). In general, it is related to cases where the contribution of the surface conduction to the overall conduction of the nanopore becomes more relevant than the bulk conduction. The ratio between effective surface and bulk conductivities is called the Dukhin length, and when this length scale is comparable to the size of the nanopore it becomes selective.[61] These surface charges present on the walls of nanopores exhibit the electric field onto the aqueous solution in contact. When the width (or diameter) of nanopore is less than roughly 2 times l_D, then the bulk properties in the center cannot be achieved even for simple electrolytes.[62] This breaking of the local electroneutrality causes ion migrations and affects the ion flow properties.[3,4] In the case when the bulk conductance of the pore is smaller than the surface conduction, the pore enters a regime where the conductance of the whole nanopore is not determined by the amount of ions available in the reservoirs but by the surface charge of the pore walls, which is tuned by physisorption and chemisorption depending on the material.[63] If the Dukhin length varies as we are moving through the pore cross section, as is the case with conical pores or pores with some sort of surface coatings, this induces ionic current rectification.[61,64] In the case of ILs, generally larger size of ions (especially large cations with longer hydrocarbon chains) will give rise to the additional selectivity for narrow nanopores. Understanding how surface conduction and bulk conduction behave in ILs and their mixtures, and what is the characteristic electrostatic lengths scale, would be the first steps to understand better the behavior of ILs in nanopores.

The experimental and theoretical study of the interface between water and ionic liquids[43,46] opens up questions regarding the interface properties. It is not clear if and how this interface impacts the slowdown of translocations, and whether just an increase of viscosity in the IL phase is sufficient to explain it. Water clustering is found to penetrate inside the ILs with ionic liquid ions being the dominant charge carriers for ion transport.[43] How this would impact, for example, ion selectivity is still unknown. One import influence on translocation velocities comes from electroosmotic flow,[65] where a mobile layer of charges inside the nanopore is being acted upon by the electric field and induces fluid flow which in turn can generate drag on a translocating analyte. Mixing of solutions of different viscosities has been indicated to produce diffusio-osmotic currents and strong electroosmotic flow with possibilities of flow reversal.[66] This effect might be related to diffusio-osmotic flows in salt gradients and the effects of low hydraulic resistance and pore edge effects in the case of nanopores in 2D materials.[67,68] One of the major questions arising here for ILs is the nature of the double layer and the effective surface zeta potential. Although electro-osmotic flow should be diminished in the ILs by the increased viscosity and high structuring inside the nanopore, it is not clear what happens when ILs is in contact with different fluid, such as aqueous solution, or other type of ILs (see Figure 1b,c). The term "interface" between partially miscible fluids is complex at thermodynamic equilibrium, not to mention our case here, where ions migrate between the two compartments. Again, the solid nanopore system is an adequate tool to better understand how mixing of miscible liquids and interfaces between immiscible liquids behave under the source of the external potential (concentration gradient, electrostatic potential, pressure).

3. DNA Translocations with Ionic Liquid and Water Interfaces

The first experimental demonstration of the slowdown of nucleotides and DNA molecules was done with a nanopore drilled in molybdenum disulfide.[46] Here, in order to compensate for the low conductivity, and thus low signal to noise level of the IL, an interface between water and the ionic liquid was established at the pore with the nucleotides dissolved in [BMim][PF_6]. This system enabled differentiation of the nucleotides based on their current drops and dwell times, and an order or magnitude or more fold slow down of lambda DNA translocation times. The proposed mechanism of the slowdown uses a simple model taking into account just the large difference in viscosity between water and the ILs (a "viscosity gradient"). The interaction with the pore wall, electrostatic interactions between the cation and the phosphate groups of the DNA and the hydrophobic association between the cation and DNA bases are also identified as possible contributing factors. [39] Recent molecular dynamics simulations indicate that the reason for this slow down might not come from ILs specific binding to the nucleotides.[43] It was found that nucleotide aggregation happens in the ILs phase with a sharp transition between the two phases at the interface, and it is this aggregation which could be responsible for the increased sensitivity to nucleotides. Albeit this does not explain the extreme slowdown of long DNA molecules as reported in the original experimental study (see **Figure 3**),[46] nor in silico results that DNA-$[BMim]^+$ ion complexation would cause similar slowdowns with graphene nanopores.[41] A modification of the pore surface charge or binding of the $[BMim]^+$ cation to the DNA were identified as possible causes of translocation slowdown with biological nanopores in aqueous solutions of a ionic liquid.[38,40] One thing is clear, ILs could provide solutions to some of the issues plaguing the advance of genome sequencing with solid state nanopores.

If ILs/nanopores systems are to be used in DNA sequencing, it is of paramount importance to avoid any damage or the fragmentation of DNA strands. Since typical ILs formulations are far from rigorous alkaline conditions, the fragmentation and damage in principle do not occur—the procedure is safe from that aspect. It must be noted that the stability of DNA helix in ILs and their aqueous solution is difficult to generalize (due to the huge variety of synthesized ILs). Detailed examination of the Hofmeister series (and inverse series) needs to be considered prior to the experiments. Effects that appear with the respect to the nature of ILs are cation binding, hydrogen bonding, solvent exclusion, base stacking, conformational entropy, and hydration.[69,70] Nevertheless, for systems such as [C_xMim][Cl], it was found that DNA duplex gains on the stability when ILs are used as a solvent, or in IL/water mixtures.[71] In general, the IL cations association to DNA is primarily governed by electrostatic interactions between cation's head groups and phosphate groups of DNA. Additionally, hydrophobic forces enhance the binding affinity for the IL cations with hydrocarbon chains, which condense to nucleotides.[72] For the same ILs in aqueous

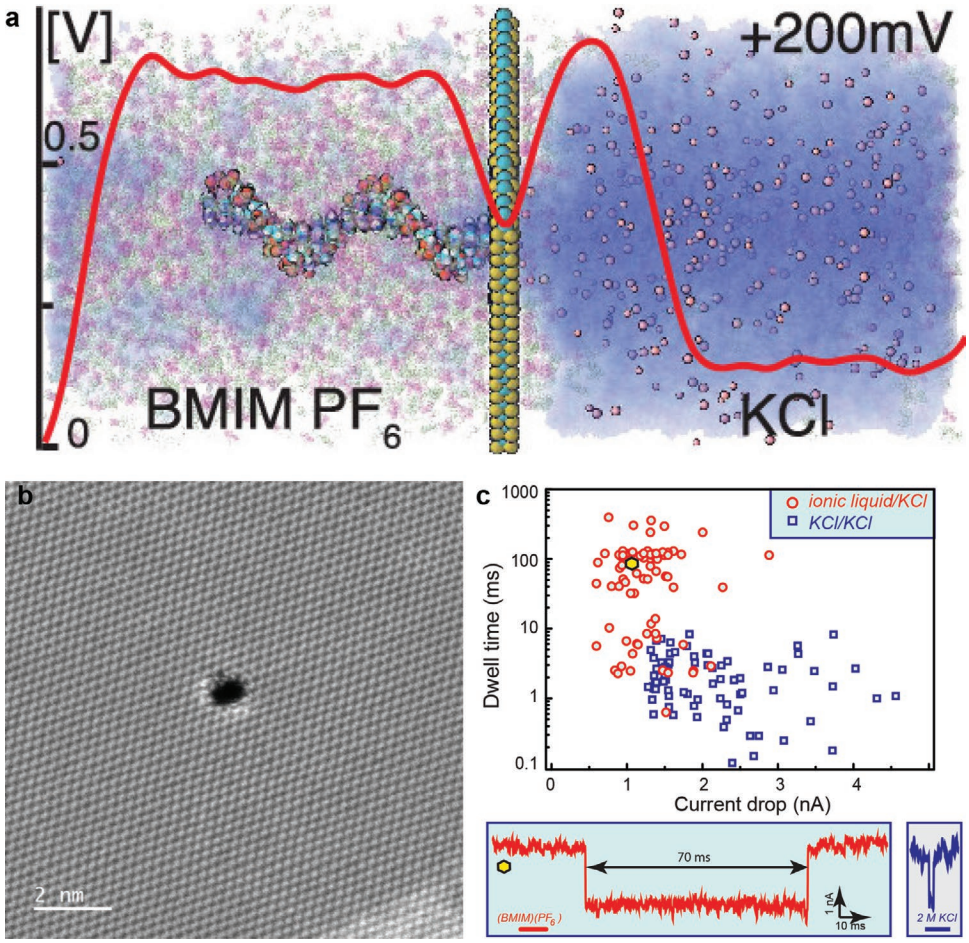

Figure 3. Ionic liquid/water interface for DNA translocations. a) A molecular dynamics simulation of a MoS_2 nanopore separating pure [BMim][PF_6] and an aqueous solution of KCl. Reproduced with permission.[43] Copyright 2021, American Chemical Society. b) Transmission electron microscopy image of a nanopore in single layer MoS_2. Image courtesy of Dr. Mukesh Kumar Tripathi. c) Example of a DNA translocation event (current vs time traces) obtained through MoS_2 nanopores. The DNA was dissolved in [BMim][PF_6] and translocated into an aqueous 2 M KCl solution as depicted in panel (a). Panel (b) represents unpublished work. c) Reproduced with permission.[46] Copyright 2021, Elsevier.

mixtures, the ions compete for the association in the grooves of DNA to exclude water molecules (water molecules tend to slightly destabilize DNA backbone).[73] Consequently, for most ILs-based systems, the degree of the denaturation is decreased.

It is known, nevertheless, that surfactants can cause coil-globule transition, so fine-tuning is needed.[74] On the colloidal scale, besides DNA folding caused by strong pressure exhibited by the external source of voltage when DNA is near the nanopore,[75] the aggregation phenomenon can also reduce the accuracy of nucleotides sequencing.[47] In the case of [C_2Mim][Cl], the ion association decreased intra-repulsions via classical Manning condensation, which led to the undesired coil-globule transition. On the other hand, in the case of [C_8Mim][Cl], the favorable overlap of the hydrophobic chains and the water exclusion caused the formation of DNA bundles which also blocked the translocation through the nanopore. It is worth noting that the optimal conditions were found for [C_4Mim][Cl] where the persistence length of double-stranded DNA was increased when compared to the two aforementioned cases. This again points to the fact that special care needs to be devoted to choosing the type of ILs for DNA detection and identification.

4. Liquid–Liquid Interface between Two Different Fluids Separated by a Solid Nanopore

4.1. Formation of the Liquid–Liquid Interface

For the system where two compartments are filled with different Coulomb fluids (e.g., ILs/aqueous solution, as in Figure 1b), it is very important to consider the miscibility of the two liquids and the establishment of the liquid–liquid (l–l) interface. For example, in ILs/aqueous solution system, ILs are in fact water saturating, due to their Coulomb nature. Saturation character is more pronounced than in biphasic water/oil systems. With ILs, water leakage is always expected due to electrostatics-based hydrogen bonding,[76] up to a threshold. This threshold is tuned by hydrophobicity of both cation and anions in the IL.[77,78]

If an IL is miscible with water throughout the entire phase diagram, no stable structuring between ILs-rich part and ILs-poor part of the system can be obtained, and the l–l interface is ill-defined. In ILs immiscible or partially miscible with water (e.g., [BMim][PF_6]), the l–l interface can form inside or at the edge of the solid nanopore, depending on the relative

wetting properties of water and the neat IL. Nevertheless, this does not mean that the l–l interface will have a strict, well-shaped boundary.

Even though mixing of IL and water is usually slow in terms of processes on nanoscale (a few hundreds of nanoseconds),[79] it is still orders of magnitude faster than ion flow between compartments, and is therefore expected to be stable during ion transport and translocation processes. However, despite the strong interest in the interfacial ILs, studies concerning l–l interface are still scarce. Nevertheless, the role of the diffuse l–l interface was demonstrated in a recent simulations on MoS_2 membrane that separates compartments with moderately hydrophobic [BMim][PF_6] and aqueous solution of KCl.[43] Simulations show that [BMim][PF_6] protrudes into the aqueous solution, while water molecules start to dilute IL compartment (see **Figure 4**a,b). Even in the absence of the electrostatic potential, the sharpness of the interface decays, contrary to the classical picture of well-defined boundary layer. Moreover, all-atom simulations reveal complete wetting of the MoS_2 surface by water molecules. The effect is preserved throughout the simulation, both with and without the imposed electrostatic potential, an effect that will be discussed later in more detail.

Surprisingly, at the l–l interface, density distribution functions show an oscillatory behavior of $[BMim]^+$ dampening toward the bulk aqueous solution (Figure 4b,d), with and without the electric field. Interestingly, K^+ ions are retained in the aqueous solution due to their strong coordinating hydration sphere. In the context of MoS_2 or other 2D materials with thickness close to a few molecular sizes,[59,80] this degree of ordering in both compartments is important. Nevertheless, we expect that for longer nanopores (larger d), especially the ones where edge effects are minor, ion flow is dominated by the fluid ordering in the interior of the nanopore. A higher degree of ordering of l–l interface and a reduced diffuse character may be established for highly hydrophobic ILs, for example, [C_nMim][PF_6] where the number $n \geqslant 8$ designates the length of hydrocarbon chain.[79]

We can conclude that the l–l interface between the aqueous phase and IL poorly miscible with water has certain characteristics of the l–l interface such as water and oil,[81,82] but due to the diffuse ion profiles and the kinetically slow phase mixing or separation, probably more intuitive term would be to refer if as "the interfacial region". Further studies are necessary to understand the properties of this region including its thickness and content. In the context of transport, this layer could have a significant influence on the diffusivity of ions and the formation of electrical double layer for a wide range of nanopores.

4.2. Transport across Liquid–Liquid Interfaces

Due to the diffuse character of l–l interface, a multitude of effects affecting solute transport and translocation may arise. Consequently the l–l interface may act both as a barrier or may promote translocation. These effects may not be small particularly if the l–l interface is in size comparable to the pore length, and if it forms at the entrance of the nanopore. The solute may structurally couple to the concentration profile of solvents resulting in concentration gradients of solutes and even ordering at nanosacale (micelles, hydrophilic nanodomains). Furthermore, the diffusivity of solutes becomes spatially dependent as it propagates through the l–l interface due to the changes in viscosity.

On the atomic scales of IL/water interfaces, in general, the water influences ILs self-diffusion coefficients, which are found to increase with increasing water content.[76,83] Namely, the addition of water in the coordination sphere of the IL's ion affects the electrostatic interactions with the ions of the opposing charge. A rule of thumb states that if the ratio of cation and anions sizes is less than 2:1, water is expected to solubilize both ions and increase their diffusivity.[84] On the other hand, if the ratio is more than 3:1, then water can associate with anions and potentially form networks of hydrogen bonds. Water will then decrease the ion diffusivity and behave as high-dielectric nanodomains known in many colloidal multiphasic liquids,[85,86] and water-in-salts systems.[87] Note that depending on the hydrophobicity of mostly cations, the trend in ionic conductivity versus

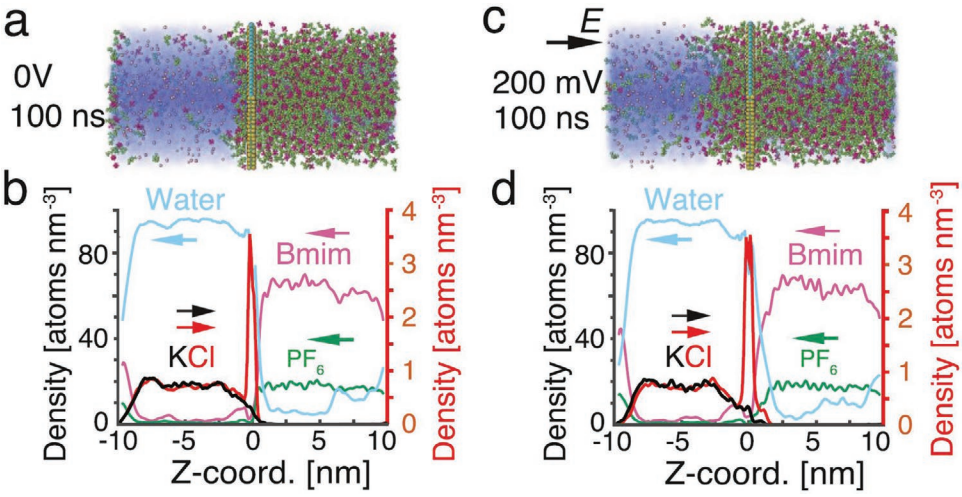

Figure 4. Simulations of [BMim][PF_6] and aqueous KCl solution compartments separated by solid MoS_2 nanopore to mimic the experimental setup presented in Figure 1b and 2b. The diffuse "interfacial region" forms beyond the MoS_2 nanopore for both 0 V and 0.2 V imposed electric potential between two compartments. Reproduced with permission.[43] Copyright 2021, American Chemical Society.

dilution can be even more complex due to self-assembly.[83] If the water content is much larger than that of IL, the viscosity within the interface region drops again causing the enhancement of ion mobilities.

Even more complex scenarios may take place with hydrophobic ILs in which case the hydrophobic part of ILs could be strongly structured at the l–l interface that may resemble the liquid crystal phase.[79] As in systems with strong amphiphiles, such as surfactants.[88] Assuming similar effects in ILs, the analyte-exchange across such l–l interface should be clearly hindered. Furthermore, in the terms of kinetics of ion transfer, a hysteresis-like behavior across the boundary is not likely, rather the diminishing of rate constant when an ion "returns" to the aqueous phase. Prior to ion return to the aqueous phase, a reorganization of interfacial layer needs to take hold, which makes this kinetically a slower process.[89] These processes are, however, still very poorly studied in ILs.

Another difficulty arises if the l–l interface forms within the nanopores, which may be the case in longer nanopore systems presented in Figure 1b,c, compared to the case of few atomic layers presented in Figure 3. If the l–l interface forms within the narrow pores,[90] ions shape and charge may play the dominant role although the latter may effectively change in the solvation gradient perpendicular to the pore wall. For l–l interfaces in thick and long nanopores (Figure 2b,c), the diffusion coefficients of ions are expected to exhibit complex trends due to the gradual increase of water concentration along and parallel to the axis of the nanopore (direction from ILs compartment to the aqueous solution) as the formation of the l–l interface competes with the liquid ordering on the pore wall.

All of the aforementioned effects are a challenge for experimental setups and for the modeling of the fluid flow.[42] Clearly, inhomogeneities at the nanoscale and the self-assembly require an integration of the colloidal chemistry aspect in a mesoscopic context.[83,91] The consequence of this spatial dependence is probably of greater importance for diffusio-osmosis (when the only driving force is the concentration gradient) than for pressure-driven devices or electro-osmosis driven systems. In later systems additional restructuring of the solvent due to the coupling with the strong electric fields may provide unisotropic changes of the solvent viscosity, and the restructuring of the ion's hydration shells affecting their diffusivity and electro-mobility.[92]

5. Interaction of Neat ILs with Nanopores

The first challenge is to understand structural properties of ionic liquids and their interplay with nanoconfinement. Due to the size of the IL ions, the intensity of the Coulomb attraction between ions carrying charge of opposing sign, and the strength of the coupling with the walls of the solid pore, the layering effects penetrate into the liquid phase on length scales that are an order of magnitude larger than in aqueous solutions.

We distinguish three regimes of pore widths. First, when the pore width is comparable to the size of IL ions (narrow pore, Figure 2b). In this case, no clear layering can take place but the structural properties of the IL are dominated by interactions with the solid.[93] In the second regime, the pore size ranges from the molecular to couple of dozens of nanometers (Figure 2c, as in the upper narrow part of conical nanopores). In this regime, clear layering of the IL will take place, the effect of which attenuates with the distance from the pore. Nonetheless, the bulk behavior of the IL may not be recovered in the center of the pore. Finally, in large pores (above ≈50 nm) the interfacial layering of IL smoothly decays to the bulk behavior. When discussing the length of the nanopore, from modeling perspective, it is important to distinguish whether the edge effects need to be included or not. Luckily this correlates with the size of the system needed for the simulation. Thinner nanopores, where the edge effects are important, can be well described by MD simulations. In contrast, mean field modeling (mesoscopic theories) are far more adequate for longer nanopores where edge effects can be neglected and correlation can be drawn by continuum modeling of flow properties.

Since the structure of the IL strongly affects the mobility of its ions, viscosity gradients develop in the interfacial region with the solid. This naturally affects all transport processes through the pore, but the quantitative studies are only in the nascent stage. Depending on the pore and analyte type, this associated conductivity may be fully dominated by surface effects or bulk effects.[94]

5.1. Structuring of Neat ILs at Solid–Liquid Interfaces

To address these challenges, a strong research effort has been developed over the last decades focusing on the understanding the interaction of the IL with the solid phase and the electrodes. Rather than in the pore, a large body of work involved IL films on solid support (**Figure 5**), due to the simplicity of the geometry and the accessibility of the interface to various experimental techniques. Using surface force apparatus in this geometry indicated that screening lengths in pure ionic liquids behave similar to dilute salt solutions although they are pure molten salts.[95] Furthermore, the steric effects of the ions were found important.[96]

However, surface force apparatus experiments showed molecular structure only on the order of several molecular layers akin to a pre-wetting layer.[97] Surface mediated ordering on even longer lengths scales has been measured with atomic force microscopy[98] and using optical techniques.[99–101] It was demonstrated that ionic liquids supported on metallic and insulating solid surfaces showed highly packed layering and ordered structures typically extend in the direction perpendicular to the substrate by several nanometers.[102–105] A similar result was obtained using X-ray reflectivity measurements.[106,107] In the structuring of the imidazolium-based ILs on neutral alumina interface, a clear checkerboard pattern was found due to the hydrogen bonding of cations and anions to the hydroxyl groups on the neutral alumina surface extending nearly 10 nm in the solution.[108]

Measurements done with a tuning fork, similar to an atomic force microscopy (AFM) also show surface mediated long range ordering of IL on large length scales.[98] Using mechanical impedance, a transition from a liquid-like response to a solid-like behavior was found at lengths of up to 100 nm from

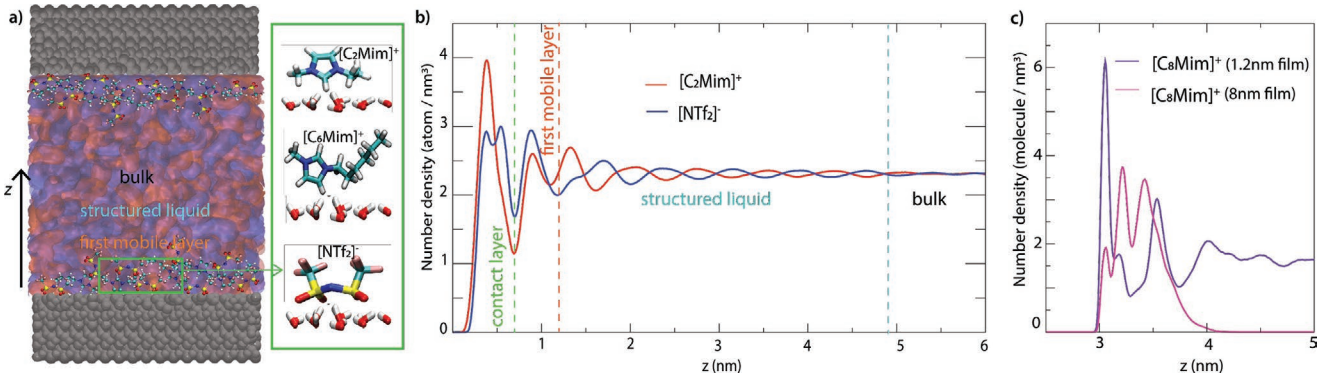

Figure 5. Interfacial properties of imidazolium-based ILs. a) Left panel: Image of a metal-oxide pore system filled with $[C_nMim][NTf_2]$. Right panel shows a typical coordination of $[C_2Mim]^+$, $[C_6Mim]^+$, and $[NTf_2]^-$ ions with the hydroxylated alumina (small red and white rods). While $[NTf_2]^-$ anion near the support is usually in *cis* configuration, the alkyl chain of cation changes form parallel $[C_2Mim]^+$ to perpendicular $[C_6Mim]^+$ to the interface. The schemes for $[C_2Mim]^+$ and $[NTf_2]^-$ are taken with permission.[111] Copyright 2021, Elsevier. b) Number density profile of $[C_2Mim]^+$ (red line) and $[NTf_2]^-$ (blue line) perpendicular to the alumina interface demonstrating strong layering in a 6 nm thick region. Reproduced with permission.[112] Copyright 2021, Elsevier. c) Number density profile per molecule of $[C_8Mim]^+$ with 1.2 nm (magenta line) and 8 nm film (purple line) demonstrating the role of the film/pore thickness on the ion stratification.

the surface. Clearly, short and long range ordering are highly dependent on the surface properties, potentially with metallic surfaces yielding the strongest effect.[98,109] This strong structuring effect on metals are presumably promoted by image charge stabilization of the IL structure, which can be, however, strongly perturbed by applying a potential to electrode.[110]

In Figure 5a, we show a model system with pore width ≈10 nm and length ≈7nm, which is directly comparable with the experimental setup that is used for application, such as DNA translocation. Adequate tool to investigate such systems are molecular modeling techniques, and in particular molecular dynamics (MD) simulations have been particularly useful in exploring the properties of the solid-IL interfaces. With MDs one important challenge is the choice of the force field.[113] Namely, most parametrizations of ILs have been developed for pure unconstrained liquids. These parametrizations may not always be successful in the context of the confinement and when recovering simultaneously static and dynamic features of the IL. This challenge was recently addressed for a nonpolarazible parametrization of imidazolium-based ILs.[112] Naturally, polarazible force field which would be developed and tested accounting for surface-sensitive measurements would be the ideal choice. However, their implementation, may come at such computational cost that they are still not feasible. Namely, it was shown that the structure of the IL in contact with the solid converges quickly, but the the following layering pattern may require over 150 ns and relatively large system size to avoid self-imaging effects.[112,114] This problem may be reduced in really thin pores, but in this case, the structure of the IL becomes extremely sensitive to the geometry and the thickness of the the pore or the thin IL film (Figure 5c).

Given that the molecular details are seldom accessible by experimental methods, molecular dynamics simulations play a key role in understanding the interplay between the IL and the solid support. However, as shown recently, in order to recover correct structuring and dynamic properties of ILs in the pore, significant computational effort and careful parametrization of the IL-solid interactions is necessary.[112] For imidazolium-based ILs in contact with mica, it is shown that small cations are mostly oriented parallel to the interface, while longer chains were oriented normal to the interface in a bilayer-like arrangement.[115] The same trends we observed also on hydroxylated alumina as shown for the $[EMim]^+$ and $[HMim]^+$ on the right panel of Figure 5a, a result that could be confirmed by infra-red[116] or X-ray photoelectron spectroscopy.[117] The simulations on the metal interfaces (Au(111)) yielded similar organization of the ions as on metal-oxides surfaces,[103,118,119] again in agreement with experiments.[120,121] Regarding long range ordering, as shown with X-ray reflectivity, the strongest effects are observed for small ions as shown in number density profiles of $[EMim][NTf_2]$ (see Figure 5b), while the structural complexity of large cations introduces disorder already 4–5 nm from the surface. Consequently, in the context of experimental setup where the nanopore is 10 nm wide, based on calculation we predict that no bulk can be formed inside nanopore, while strong layering will dominate both static and dynamic properties of this system. This is all the more reason why layering and structuring properties of ILs in nanopores should be connected with surface and bulk conductance to achieve optimal condition for slower ion migrating between the two compartments (Figure 1).

Despite the fact that most quantitative experiments and simulations consider film-like geometries, there is a considerable effort to address true porous systems. However, in this case, the geometry and pore distribution must be taken into account while interpreting the data. Some valuable information emerged so far. For example, in porous alumina membranes IL glass temperatures have been shown to increase below a critical confinement size, but the functionality is also dependent on the length of the imidazolium cation length of the chain.[122] As observed in supported IL films (see Figure 5c), larger chains showed less restrictive confinement. MD simulations of neat ILs in confined in silica nanopore showed that ILs maintain liquid-like structure close to the interface, most likely because the melting point decreases upon confinement.

5.2. Transport in the IL-Filled Pore

The field of nanofluidics is known to show many interesting behaviors regarding ion and fluid transport. The main reason for such phenomena lies in the comparability of several physical lengths scales with the objects under study.[4] Bjerrum length is the measure when the relative strength of the electrostatic interaction between ions is comparable to the thermal energy in the system. In the case of ionic liquids, due to their lower relative dielectric constants[123] it will be an order of magnitude larger than its value of 0.7 nm for water-based solutions. The electrostatic screening length, a measure of how ions collectively screen each other, is usually found to be in the range of 6–9 nm for typical ionic liquids or extremely concentrated salt solutions in water,[95,124–126] comparable to a 1 mM KCl solution in water. But, the peculiarities of ionic liquids come from the interplay of long range electrostatics, strong dipole–dipole interactions and sterics, leading to more complex behavior on the nanoscale.

The strong density oscillations and the appearance of glassy states discussed in the previous section strongly affect the driven and diffusive mass transport in the nanopore.[127] Furthermore, the ionic nature of the liquid and its delocalized charge enable complex scenarios for the charge transfer.[126] The velocity of translocation of analytes is likely to be coupled with the clustering of ions.[128] However, the understanding of these processes are still in the nascent stage.[43]

So far, it is relatively well accepted that for the majority of ILs, the cation is more diffusive than the anion.[129] In the case of imidazolium-based cations, it was shown that the motion of the tails is notably faster than that of the imidazolium rings, as well as anions.[130] Due to that effect, mobility of polar and nonpolar region can be crucially different.[131] However, to understand the transport of dissolved species in the pore, it is necessary to gain good knowledge of viscosity modulations within the pore. Nonetheless, fully grasping the relation between structure and diffusivity of IL has been a real challenge and requires precise analysis of the single pore transport.

Measurements in single pores are, however, scarce due to the drop in signal to noise level as compared to multi-pore membranes and the complexity of handling pure ionic liquids. Namely, the high viscosity (often 10–100 times that of water) considerably slows down the IL imbibition. Standard procedures based on alcohol pre-wetting are not convenient in the case of ILs because an amphiphilic film may form on the nanopore surface.[132] In addition, while the low vapor pressure of the IL allows for the extensive degassing of the sample under vacuum, this requires changes in the classical open sample chambers commonly used in the field. If the membrane resistance is lower than the pore resistance, it will cause the current to preferentially flow through the substrate material bypassing the nanopore. Therefore, as discussed in Section 2, the pore for transport measurements must be built from high-resistance materials such as intrinsic silicon, fused glass chips,[133,134] or conical shaped glass nano-capillaires.[48] Besides preparing the sample, further difficulties arise with accurate measurements of conductivity due to the high resistivity of measurement techniques and nanopore membranes with low leakage.[135]

First measurements of single pores showed a sharp increase in resistance of pores below ≈50 nm,[44] yet it was not possible to associate these observation to wetting issues or freezing effects. A somewhat conflicting results were obtained from measurements of transport coefficients in single conical pores. Here, the data showed little dependence on the size range of 20–800 nm.[48] This is postulated to be due to a number of possible reasons ranging from contamination of IL with water known to change structural properties,[51,136] to a poor system reproducibility. Another study found that some ionic liquids produced a lower level of flicker noise in nanopores,[45] attributing it to a lower level of charge fluctuations inside the nanopore.

From the modeling perspective, the most effort was associated with determining the diffusion parallel to the pore IL.[137–140] Given that the symmetry of the system is preserved over this axis, self-diffusion coefficients may be obtained from mean square displacement (Einstein approach)[141] or the velocity autocorrelation function (Green–Kubo formalism).[142] It was shown that ions at the solid–liqud interface may strongly coordinate with particular moieties on the surface, which may impede their free diffusion (see **Figure 6**a). This effect is

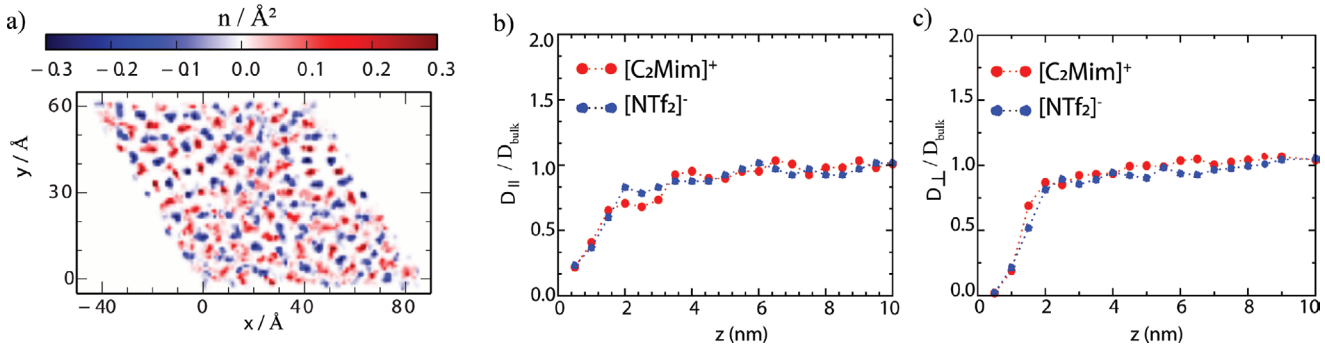

Figure 6. Diffusion properties of $[C_2Mim][NTf_2]$ close to the interface of an alumina pore. a) The 2D density map of the centers of mass accumulated over 50 ns MD simulations of all ions in contact with the surface (cations shown in red, anions in blue). Besides a checkerboard-style, a strong suppression of diffusivity is observed due to hydrogen bonds with between the ions and the surface. b) The lateral $D_{||}$ and c) the perpendicular $D_{\perp}$ diffusion coefficients of $[C_2Mim]^+$ (red) and $[NTf_2]^-$ (blue) as a function of the distance from the alumina surface. In the first double-layer, the ions are more mobile parallel to the interface. However, the bulk values are attained slower and the correlations with density stratification are more significant. $[C_2Mim]^+$ corresponds to, for example, EMim. Adapted with permission.[112] Copyright 2021, Elsevier.

stronger for small cations, as shown for the imidazolium-based ILs. This slow-down is also seen in the immediate following layers of IL where diffusion coefficients maybe an order of magnitude smaller than those in the bulk (see Figure 6b). Since mobility of ions shows a strong correlation with the effects of structuring and layering, the bulk values can be obtained only in the regions where the structure of the fluid in the film is indeed that of the bulk liquid.[112] Another study showed the relation between fast (or slow) diffusivity during charging and dense (or loose) ion packing inside the pore.[143] If the pore is narrow enough, the bulk liquid should to be observed in the pore, and the mobility of the ions should drop with increasing level of confinement.[114] Interestingly, it was suggested that if the pore is so narrow such that it contains only one layer of ions, their diffusivity may increase during charging and exceed the bulk diffusion value. The diffusivity in wider pores is independent of the charge.[144]

For the components perpendicular to the pore, the anisotropy has to be addressed directly, on the level of the model for extraction of the diffusion coefficient. This was first done using the so-called Jump-diffusion model.[145] According to this method, the system is first divided into slabs parallel to the interface. In the following, the average lifetime of the ion in a particular slab is heuristically related with the self-diffusion coefficients perpendicular to the slab boundaries. Unfortunately, the direct application of that model to the IL data from molecular dynamics (MD) simulations leads to an order of magnitude large discrepancy between the estimated diffusion coefficients and the ones obtained from the mean square displacement, even in bulk conditions.[112] Accurate determination of diffusivities in the film requires a more detailed statistical treatment and taking into account the fact that the average shape of the ion changes throughout the pore (see Figure 6c)

6. Interaction of Diluted Ionic Liquid and Solid Surface

Interaction of the solid pore with the diluted solution of IL in water may introduce complex stratification effects. The structure at the solid–liquid interface depends on relative hydophobicities of the ions which compete with water with their own affinity for the solid surface. Besides the nanopore ionophobicity character, the degree of crystallinity is an important factor on ion transport as well.[90] Depending on the interplay between these interactions, there are several possible outcomes.

As was seen in Figure 4, the wetting of the nanopore is important effect on both molecular scales and the nanoscale. In the context on nanopores, one of crucial effects of mixing water and IL is the change in the wetability of the pore, and the restructuring of the IL density profiles.[146,147]

In the context of wider nanopores, such as 10–20 nm silicon nitride or in middle-to-upper part of conical nanopore (Figures 2b and 2c, respectively), an interesting finding is that by following the phase diagram of bulk water content in the mixture, ILs (both [BMim][BF_4] and [EMim][BF_4]) show complex landscape of behavior, from acting as a solvent for low $x_{H_2O} < 0.3$, co-solvent for $0.3 < x_{H_2O} < 0.9$, and as solute at $x_{H_2O} > 0.9$.[148] This is especially important since we already mentioned that in two-compartment system separated with nanopore, we might expect diffuse "interfacial region" of varying x_{H_2O}, thus all of the three ILs colloidal behaviors imply, and need to be accounted for. In this nanopore width regime, it is needed to note that concentrated salt solutions exhibit long-range correlations between ions (the correlation length)[57,149] and solid surfaces (the screening length).[124] It appears that in concentrated systems, the interactions between all ions and surface (the nanoconfinement) span way beyond typical Debye decay length, which becomes very small for these conditions.[58] Consequently, the system is not dominated by the thermal motion (the entropy), but rather gains some sort of ordering. Apart from concentrated solutions of 1:1 electrolytes, similar behaviors are observed and theoretically reproduced for ionic liquids systems,[56,150] or biphasic aqueous systems.[151] Theoretical predictions are up to now valid quantitatively for Debye dilute concentration regime, and beyond that on a qualitative level. Nevertheless, an increase in the correlation and the screening lengths are predicted with an increase of concentration. Although already complicated, a system of two compartments with different Coulomb fluids faces this property as well.

6.1. Hydrophilic and Hydrophobic Surfaces with Water/IL Mixtures

Hydrophyilic interfaces will promote adsorption of water which is furthermore enhanced by the potential hydrophobicity of the IL ions. If water occupies a significant fraction of the surface, it will sterically prevent the access of the ILs to the solid. Furthermore, water will coordinate with the surface to counteract locally the polarizing field of the support, in essence screening the surface.[152] The combination of these effects can cause an increase in the ion diffusivity and create an excess of "mobile" ions that can contribute to the overall ion flow.[153] The aforementioned effect is pronounced for narrow and long nanopores (see Figure 2b), but it can span for widths up to few dozes of nanometers, depending on the nature of IL.

An example of this mechanism on molecular scales was demonstrated by simulations of mildly hydrophilic silicon surface in contact with ILs/water mixtures, where no external electrostatic potential was applied.[148] The water content in the surface layer was calculated as a function of the hydrophobicity of ILs (see **Figure 7**a). Despite being miscible in water, structuring on 1 nm lengths or more from the solid surface was observed. The fraction of the adsorbed water $K_{H_2O}(\Delta)$, showed the expected increase with respect to the water mole fraction in the bulk (x_W) for all ILs. The amount of the adsorbed water increased in the case of more hydrophilic IL, as, for example, [EMim][BF_4] compared to [BMim][BF_4] (larger hydrocarbon chain). This is because the water molecules were able to penetrate the interfacial layer to form many-body interactions (Keesom) with both anions of [EMim][BF_4] and the interface itself.[147,154,155]

If, however, ions condensate on the surface of the solid due to attractive van der Waals interactions, as in the case of hydrophobic carbon electrodes, graphene supercapacitors, or carbon nanotubes,[156] water will be displaced

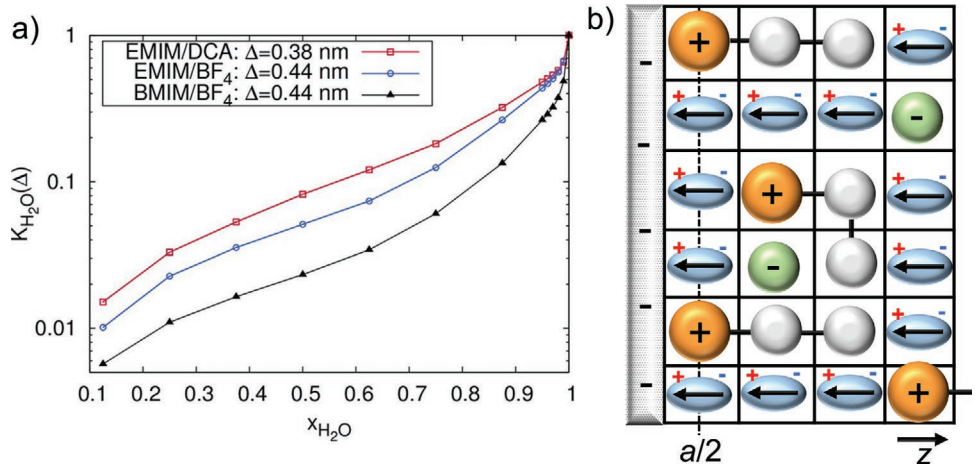

Figure 7. Effect of water adsorption onto hydrophilic surface with no applied voltage. a) Fraction of water molecules $K_{H_2O}(\Delta)$ within distance Δ from the surface, as a function water mole fraction x_{H_2O} in the bulk IL/water mixture. Δ corresponds to the first minimum of the local total particle density (ion and water molecules). The three cases of ILs are presented, based on their hydrophobicity properties. Reproduced with permission.[148] Copyright 2021, American Chemical Society. b) Schematic representation of mean-field lattice model for ILs/water mixture ($0.5 < x_{H_2O} < 0.8$) in contact with negatively charged surface. Cations are represented with orange, hydrocarbon segments with grey, anion with green, and water molecules (dipoles) with blue color. Connectivities between hydrocarbon segments are depicted with black lines. *a* is the cell size where particles are placed, and can be approximated as Δ in (a). Water molecules give rise to medium polarization and condense to the hydrophilic surface. Ions are displaced toward the bulk, so that more "charge carriers" are available. Hydrocarbon apolar segments tend to self-assembly via van der Waals forces. $a/2$ designates the closest approach of ions, while partial charge of adsorbed dipoles can still contribute to the screening of the surface charge on the "left" of the mid-plane.

toward the bulk.[147,157] Stabilization of water in wider nanopores, especially in hydrophobic ILs is then achieved by its aggregation into condense nanodomains or networks of hydrogen bonds.[158] Due to the aggregation phenomenon and ions condensation to the solid, a decrease of ions diffusivity is expected, thus the reduction of the ion flow between two compartments.

While the molecular structuring can be understood using surface sensitive measurements or molecular dynamics simulations, the formation of the double layer and structures that appear on longer time scales are susceptible to mean field modeling and in particular to the classical density functional theory (cDFT).[16,159] Water may be treated both implicitly[160] and explicitly[161] with very low computational cost although, ILs should be completely miscible in the entire phase diagram. Under these conditions cDFT can provide an estimate of the amount of the adsorbed water onto nanopore walls (see Figure 7b) if explicit water models, such as Langevin dipoles are considered.[162] At the same time, the polarization effect of the IL/water mixture and the crowding effects near the interface can be decoupled from structure nearing the surface layer. Consequently, the average EDL formation and the inhomogeneities of ions and water densities perpendicular to the nanopore axis can be considered by accounting for the ion/surface van der Waals and image charge effects to fit the hydrophobicity/hydrophilicity properties,[163] as shown for complex water-in-salts systems.[164] This approaches were tested versus experimental measurements of supercapacitor capacitance, and they can be generalized for different nanopore geometries.[165] Nevertheless, although very powerful, these theories still require finding complex algorithm solutions to obtain accurate mean field potentials.

6.2. Non-Aqueous Mixtures

Similar ion response was found also in mixtures of ILs with organic solvents.[166–168] For example, IL ions displayed an increase diffusivity in mixtures with acetonitrile, affecting the capacitance of the carbon nanopores. The solvent effect as crowding of the interface and partial solvation of ions is common for polar organic solvents, and in principle can serve as a commodity in design for efficient ion flow between the two compartments.

Although interesting with respect to phase space properties,[76,169] ILs/aliphatic alcohol mixtures are not really desirable since many alcohols behave as weak surfactants and will bind to a wide range of solid materials to form monolayers due to its amphiphilic nature. Upon adsorption to solid surface, aliphatic alcohols can sterically weaken ILs interactions with nanopore surface. Also, their amphiphilic character (in particular, aliphatic alcohols are more hydrophobic than ILs ions) will cause a diversity of self-assembly which are difficult to manage experimentally,[170] and even more difficult to predict theoretically.[171] If the idea is to slow down the flow of ions between the two compartments, then ILs ordering at nanopore walls should not be prevented completely. Also, the solubility vapour pressure issues reduce the flexibility of the experiment's design.

6.3. Transport and Translocation through Confined Diluted IL Solutions

While transport in water filled solid state nanopores has been discussed extensively, mixtures with ILs are only starting to be considered. However, if the first challenge is overcome and the

static properties of IL/water mixture are well defined, the transport and translocation through the nanopore can be obtained in the simplest manner by introducing the free energy functional into continuity equation to obtain the flux of ions[172,173] or other appropriate mesoscopic numerical model. This approach seems to be more successful for dilute solutions than for neat ILs.[174] This is thus an interesting venue that should be explored more systematically in the future including the validation with experiments.

So far, it was shown that dielectric of water as medium decreases with increasing confinement.[175] This work also offered a viable route to decipher the measured current in the nanopore into main charge carriers,[173] the identification of which is still an open question in water diluted ILs. Furthermore, for nanopores with the width comparable to the molecular size of the solutes (of few molecular sizes), the solvent layering effects still require studying the structural stratification of the solute and the dependence of its mobility on the distance from the pore wall. cDFT could be particularly useful in this direction as it allows for the inclusion of shape anisotropy as well as charge delocalization .[176–178] This may be pertinent in systems involving highly hydrophobic ILs. While these are all steps forward, the rigorous treatment of transport in confined diluted ILs is still subject to an open debate both from the experimental and modeling points of view.

7. Outlook

The usage of the room temperature ionic liquids in nanopore setups would be a big shift from classical aqueous solutions, as is evident from a low number of papers published within the community.[44–48] In order to make this novel field more approachable, we have used analogies to the well understood behavior in aqueous solutions. Our understanding of these systems is still in its infancy, so such analogies should be taken only as a guideline for future research. Even more challenging may be systems combining aqueous and IL solutions.

The idea is that the aqueous solution supports high currents through the nanopore, while the high viscosity and possibly structural ordering of ILs support the slowdown of translocating analytes. However significant effort in understanding the driving interactions and flow phenomena are necessary before this system reaches practical application.

In their pure form (neat), ILs are similar to dilute aqueous solutions in terms of typically low conductance due to ion pair formation,[179] but have characteristics of concentrated aqueous systems, such as high viscosity and large screening lengths.[57] It follows that, when water is used as a solvent, only pores with diameters below few nanometers could be used to probe the influence of sterics and ion solvation on ion conductance when water is used as the solvent. However, the Bjerrum length in neat IL is an order of magnitude larger than in water due to strong correlations and the size of constitutive ions, contrary to the Debye length which is smaller than the ion size. An equivalent of solvation effects should be seen in significantly larger pores due to the long range of electrostatic interactions.[80,180,181] In addition, in ILs the size, the shape anisotropy, and the charge localization[182] all affect the ion solvation, and thus also any electrokinetical phenomena. Hence, the choice of ILs may be utilized to design more advanced and controllable functionalities of the nanopore. For example, the nanometer thin pores filled with ILs can rely on steric effect of individual IL ions to support high levels of translocated ion selectivity.

Solid state nanopores are furthermore an ideal device to study the formation of interfaces between IL and the solid or another liquid. In this context, nanopores could be used as single molecule devices measuring free or controlled translocation[20] or streaming currents.[65] Besides strong structural correlations at the interface, which strongly couple to transport, IL often supports the formation of pseudo-phases in mixtures, micellization,[91,182] and clustering. The role of ion clustering as well as the mechanism for ion transport could be probed using nanopore systems as a bottleneck for ion transport based on the cluster size.[128] Despite these recent efforts, the question how the long range electrostatic interactions, ordering, and hydrophobic self-assembly are influenced by the solid pore is still not resolved, particularly in the context of confined aqueous solutions of ILs.

Even though the task associated with controlling the long range correlations in ionic liquids, both in neat and diluted states, is very demanding, we see this as an exciting opportunity to access the rich diversity of functionalities for nanofluidic devices arising. Manipulating the choice of ILs, the size and the functionalization of the pore and the thermodynamic conditions in a systematic manner is the key to obtain reliable trends. While the work performed so far can be seen as promising, it is clear that mastering this system requires a significantly better understanding of the formation of liquid–liquid (IL-IL, or IL-aqueous solutions) and solid–liquid interfaces (neat and dilute ILs with the solid pore). This requires a synergistic theoretical and experimental effort on both molecular and colloidal scales to decipher the relation between static and dynamic properties of interfacial ILs. However, both experimental and theoretical approaches require further methodological development to achieve the accuracy necessary for the unambiguous identification of relevant effects.

From experimental point of view, main challenges lie with the preparation methods, particularly to achieve a fully reproducible pore geometries, chemical functionalization, and the control of defects. Compared to water, ILs are more viscous, which makes the filling of nanopores harder, thus requires the development of new experimental protocols. An added bonus is that ILs do not evaporate, making experiments using vacuum and degassing more approachable. On the other side, the presence of solvent in all types of ILs mixtures, drastically changes both bulk and interfacial properties. Notably, apart from acting as a solvent or co-solute,[183] water may be considered as an impurity due to the hygroscopicity of neat ILs. Experimental characterization of the interfaces within the pore is another challenge, where novel measuring techniques need to be developed that can simultaneously address static and transport properties on different time and length scales.

The involvement of many scales in the time and spatial domain is also a challenge from the theoretical point of view, yet it is an exciting perspective for the establishing new tools. Namely, the molecular modeling is well established to study

the behavior of confined liquids with the atomic resolution, but the parametrization of the interactions at interfaces, as well as the extraction of dynamic properties of solvents and solutes in confinement requires further developments. The transport is however well studied using mean field and mesoscopic methods, yet, in this case the long-range and many-body correlations must be dealt with to achieve the necessary accuracy. Potentially perspective lies in hybrid approaches where the mesocopic models can integrate the information from the atomistic scale. A suitable tool for this line of research are lattice Boltzmann electrokinetics (LBE) simulations,[184–187] which can now also account for the catalytic and heat flows[188] and nanocapacitor properties.[187] LBE offer the possibility of accounting for electro-osmosis driven flow of ions along the axis of the nanopore of a broad range of sizes and geometries, while simultaneously accounting inhomogeneities of ions and solvent distributions perpendicular to the ion flow between the two compartments.[105] This can be especially important for modeling of flow properties in the case of two compartments with different Coulomb liquids where the "interfacial region" is always present.

The acquisition of appropriate methodologies and developing the understanding of the fundamental driving forces of transport in IL-filled nanopores opens a wealth of perspectives in utilizing these systems as a new technology. One of the major applications for neat IL in nanopores could be in the nucleic acid purification, storage, and sequencing, where the high viscosities and structural ordering, chemical properties, and stability of the IL could aid in the the slowdown of translocations, and at the same time facilitate extraction and storage of DNA, respectively. Besides demonstrated ILs potential for DNA preservation and extraction,[189–191] interactions of ILs with RNA were used to facilitate purification and to protect RNA molecules from degradation caused by Ribonuclease (RNase I).[192] Improving the stability and extraction of RNA is particularly important as it might lead to the development of more robust and accurate diagnostic tools for the current and future pandemics. The extremely low vapor pressures of ILs makes these liquids better solvents than water for applications that deal with low volumes. Hence, the low-volume nucleic acid devices (nanopores, nanofluidics/microfluidics-based biosensors, etc) should generally last longer and be reusable for multiple cycles in ILs.

In the context of single molecule nanopore experiments, so far only translocation and discrimination of single nucleotides in water-IL interfaces has been demonstrated using 2D materials,[46] with the question if aggregation was one of the mechanisms responsible for the sought off slowdown of translocations. Answering these questions would require more targeted studies of the influence of IL on nucleic acids to understand which specific types are interesting candidates for experiments. Another interesting property of ionic liquids is that their viscosity/friction could be tailored with an applied external potential (electric field).[98,193,194] If the local ordering in ILs could be harnessed, it would provide a way to control the local viscosity in the pore and slow down DNA translocations sufficiently to use solid state nanopores for DNA sequencing if it could be balanced with the required signal to noise ratio.[21,28] We envisage the possibility to use transverse electric fields to modulate the

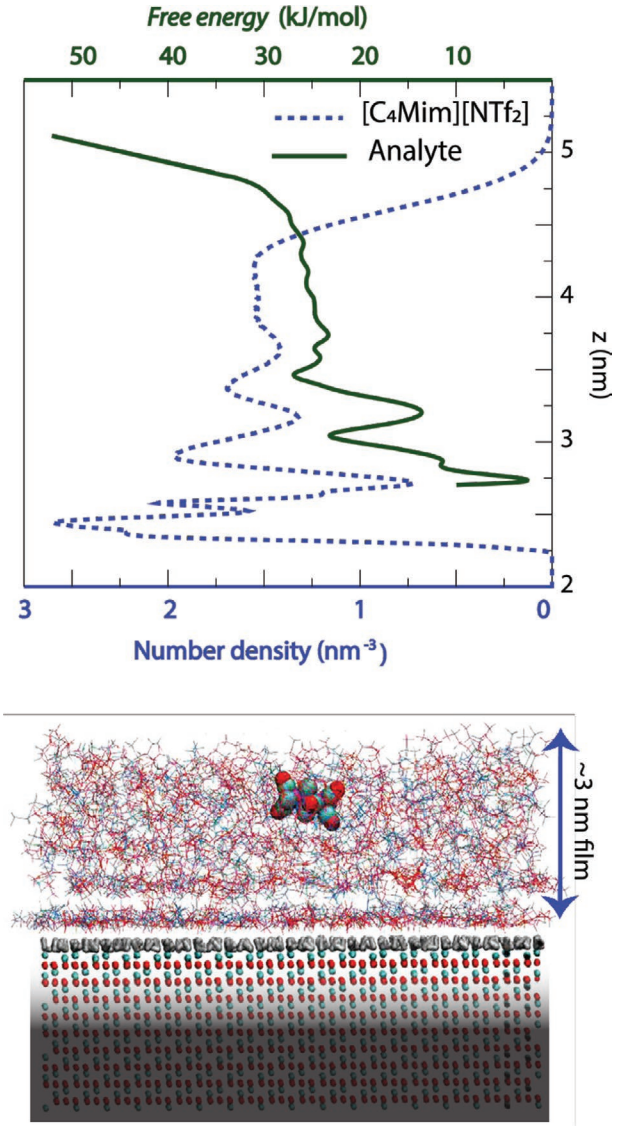

Figure 8. Potential of mean force for a ruthenium-based nanoparticle (green) and the density distribution of the IL film (blue). In this case, a strong correlation between low density regions in the IL and the minimum in the potential between the particle and the alumina can be observed. Note that $[C_2Mim]^+$ corresponds to $EMim^+$, $[C_6Mim]^+$ to $HMim^+$, and $[C_8Mim]^+$ to $OMim^+$, respectively.

degree of ordering of nanoconfined ILs,[2] possibly even controlling the freezing or unfreezing of the ionic liquid during a translocation event. Geometries like in the case of transverse DNA translocation detection[26,135,195,196] could provide such additional transverse electric fields to induce local ordering in the pores as well as being a possible aid in the gating properties of the 2D material itself. Here, thicker membrane materials would support higher degrees of ordering due to more pronounced interactions with the solid interface so that geometries like membrane embedded electrodes like in the case of ionic field effect transistors might provide better control.[197,198] Also, there are other interesting systems where the slow down of nucleotides could be achieved using phase separation. Aqueous solutions of lithium bis(trifluoromethanesulfonyl)imide

(LiTFSI) salts and stable biphasic water-in-salt systems are also candidates due to higher viscosity, and liquid–liquid interface properties.[151]

Although for slowing down DNA translocations the combination of high viscosity and low conductance is in competition, for advanced ionic functionalities this might not be a issue. The high ILs viscosities would imply less of an influence of electroosmotic flow and allow for necessarily excluding complex nonlinear ion transport functionalities arising due to a competition of advective and diffusive ion transport.[52,199] As IL ions have lower diffusion constants and higher viscosity than water solutions, the Péclet number is still reasonable such that interesting nanofluidic phenomena may take place in a temperature-dependent fashion.

Finally, we have shown that the combination of ionic liquids with solid state nanopores as single molecule devices provides a unique system where basic properties of thermal and non-equilibrium transport can be studied in great detail with the aim of understanding static and dynamic correlations of the confined liquid and of the solutes. This system provides an unprecedented access to a number of fundamental questions outlined in this article, yet addressing them will require strong methodological advance in experiments and modeling techniques. Furthermore, solid state nanopores are equally exciting from the technological point of view. In this context, a proof of principle is established that using nanopores with ILs and the aqueous salt solution one can get the best of both worlds for slowing down of nucleotides translocations, potentially allowing a reliable readout of DNA sequence. However, this is only one possible application of IL-filled nanopores. Given its richness in physics and the technological importance, we are convinced that this emergent system will be in focus of many studies in the years to come.

Acknowledgements

S.M. and N.V.-A. contributed equally to this work. The authors thank Dr. Mukesh Kumar Tripathi and Prof. Andras Kis for high-resolution TEM images of MoS_2 nanopores. The authors thank K. Hüllring for providing **Figure 8**c. M.Š. and A.S.S. acknowledge the Ministry of Science and Education, Republic of Croatia support through Klasa640-02/19-04/00145 URBROJ 533-03-19-0002. M.Š. received additional support through EIT Climate - KIC for Alumni Micro-award grant. N.V.A. was funded by the Croatian Science Foundation grant DOK-2015-10-9140. A.S.S. and N.V.A. acknowledge the project M2 within the SFB 1543 Catalysis at Liquid Interfaces funded by the German Science Foundation at the FAU. S.M. and A.R. acknowledge support by the Swiss National Science Foundation under award no. BIONIC BSCGI0 157802. The positioning of Figures 3 and 4 was amended on May 13, 2021, after initial publication online.

Conflict of Interest

The authors declare no conflict of interest.

Keywords

ionic liquids, nanopores, translocations

Received: February 5, 2021
Revised: April 1, 2021
Published online: May 6, 2021

[1] C. Dekker, *Nat. Nanotechnol.* **2007**, *2*, 209.
[2] S. Zhang, J. Zhang, Y. Zhang, Y. Deng, *Chem. Rev.* **2017**, *117*, 6755, pMID: 28032993.
[3] R. B. Schoch, J. Han, P. Renaud, *Rev. Mod. Phys.* **2008**, *80*, 839.
[4] L. Bocquet, E. Charlaix, *Chem. Soc. Rev.* **2010**, *39*, 1073.
[5] T. Mouterde, A. Keerthi, A. R. Poggioli, S. A. Dar, A. Siria, A. K. Geim, L. Bocquet, B. Radha, *Nature* **2019**, *567*, 87.
[6] I. Vlassiouk, S. Smirnov, Z. Siwy, *Nano Lett.* **2008**, *8*, 1978.
[7] R. C. Rollings, A. T. Kuan, J. A. Golovchenko, *Nat. Commun.* **2016**, *7*, 1.
[8] Z. Siwy, A. Fuliński, *Phys. Rev. Lett.* **2002**, *89*, 4.
[9] Z. Siwy, I. D. Kosińska, A. Fuliński, C. R. Martin, *Phys. Rev. Lett.* **2005**, *94*, 048102.
[10] J. R. Werber, C. O. Osuji, M. Elimelech, *Nat. Rev. Mater.* **2016**, *1*, 1.
[11] M. Macha, S. Marion, V. V. R. Nandigana, A. Radenovic, *Nat. Rev. Mater.* **2019**, *4*, 588.
[12] E. Knipping, C. Aucher, G. Guirado, L. Aubouy, *New J. Chem.* **2018**, *42*, 4693.
[13] X. Wang, M. Salari, D.-e. Jiang, J. Chapman Varela, B. Anasori, D. J. Wesolowski, S. Dai, M. W. Grinstaff, Y. Gogotsi, *Nat. Rev. Mater.* **2020**, *5*, 787.
[14] M. Galiński, A. Lewandowski, I. Stepniak, *Electrochim. Acta* **2006**, *51*, 5567.
[15] M. Armand, F. Endres, D. R. MacFarlane, H. Ohno, B. Scrosati, *Nat. Mater.* **2009**, *8*, 621.
[16] M. V. Fedorov, A. A. Kornyshev, *Chem. Rev.* **2014**, *114*, 2978.
[17] F. Zhou, Y. Liang, W. Liu, *Chem. Soc. Rev.* **2009**, *38*, 2590.
[18] C. Chiappe, D. Pieraccini, *J. Phys. Org. Chem.* **2005**, *18*, 275.
[19] S. Keskin, D. Kayrak-Talay, U. Akman, Ö. Hortaçsu, *J. Supercrit. Fluids* **2007**, *43*, 150.
[20] M. Wanunu, W. Morrison, Y. Rabin, A. Y. Grosberg, A. Meller, *Nat. Nanotechnol.* **2010**, *5*, 160.
[21] D. Branton, D. W. Deamer, A. Marziali, H. Bayley, S. A. Benner, T. Butler, M. D. Ventra, S. Garaj, A. Hibbs, S. B. Jovanovich, P. S. Krstic, S. Lindsay, X. Sean, R. Riehn, G. V. Soni, V. Tabard-cossa, M. Wanunu, *Nat. Biotechnol.* **2008**, *26*, 1146.
[22] V. Marx, *Nat. Methods* **2015**, *12*, 1015.
[23] J. Kasianowicz, E. Brandin, D. Branton, D. Deamer, *Proc. Natl. Acad. Sci. U.S.A.* **1996**, *93*, 13770.
[24] L. Zhou, K. Li, Z. Li, P. He, K. Lin, J. Mo, J. Ma, *J. Vac. Sci. Technol. B, Nanotechnol. Microelectron.: Mater. Process. Measure. Phenomena* **2019**, *37*, 061809.
[25] P. Goyal, P. V. Krasteva, N. Van Gerven, F. Gubellini, I. Van den Broeck, A. Troupiotis-Tsaïlaki, W. Jonckheere, G. Péhau-Arnaudet, J. S. Pinkner, M. R. Chapman, S. J. Hultgren, S. Howorka, R. Fronzes, H. Remaut, *Nature* **2014**, *516*, 250.
[26] F. Traversi, C. Raillon, S. M. Benameur, K. Liu, S. Khlybov, M. Tosun, D. Krasnozhon, A. Kis, A. Radenovic, *Nat. Nanotechnol.* **2013**, *8*, 939.
[27] D. Garoli, H. Yamazaki, N. Maccaferri, M. Wanunu, *Nano Lett.* **2019**, *19*, 7553.
[28] B. M. Venkatesan, R. Bashir, *Nat. Nanotechnol.* **2011**, *6*, 615.
[29] U. F. Keyser, B. N. Koeleman, S. van Dorp, D. Krapf, R. M. M. Smeets, S. G. Lemay, N. H. Dekker, C. Dekker, *Nat. Phys.* **2006**, *2*, 473.
[30] H. Peng, X. S. Ling, *Nanotechnology* **2009**, *20*, 185101.
[31] G. M. King, J. A. Golovchenko, *Phys. Rev. Lett.* **2005**, *95*, 216103.
[32] S. Huang, J. He, S. Chang, P. Zhang, F. Liang, S. Li, M. Tuchband, A. Fuhrmann, R. Ros, S. Lindsay, *Nat. Nanotechnol.* **2010**, *5*, 868.
[33] D. V. Verschueren, M. P. Jonsson, C. Dekker, *Nanotechnology* **2015**, *26*, 234004.
[34] Y. He, M. Tsutsui, R. H. Scheicher, C. Fan, M. Taniguchi, T. Kawai, *Biophys. J.* **2013**, *105*, 776.
[35] N. Di Fiori, A. Squires, D. Bar, T. Gilboa, T. D. Moustakas, A. Meller, *Nat. Nanotechnol.* **2013**, *8*, 946.

[36] M. Waugh, A. Carlsen, D. Sean, G. W. Slater, K. Briggs, H. Kwok, V. Tabard-Cossa, *Electrophoresis* **2015**, *36*, 1759.
[37] V. A. Bloomfield, *Biopolym.: Orig. Res. Biomolecules* **1997**, *44*, 269.
[38] R. S. S. de Zoysa, D. A. Jayawardhana, Q. Zhao, D. Wang, D. W. Armstrong, X. Guan, *J. Phys. Chem. B* **2009**, *113*, 13332, pMID: 19736966.
[39] Y. Ding, L. Zhang, J. Xie, R. Guo, *J. Phys. Chem. B* **2010**, *114*, 2033, pMID: 20088558.
[40] D. A. Jayawardhana, J. A. Crank, Q. Zhao, D. W. Armstrong, X. Guan, *Anal. Chem.* **2009**, *81*, 460.
[41] M. Kulkarni, A. Mukherjee, *RSC Adv.* **2016**, *6*, 46019.
[42] X. Jiang, Y. Liu, R. Qiao, *J. Phys. Chem. C* **2016**, *120*, 4629.
[43] M. Shankla, A. Aksimentiev, *ACS Appl. Mater. Interfaces* **2020**, *12*, 26624.
[44] M. Davenport, A. Rodriguez, K. J. Shea, Z. S. Siwy, *Nano Lett.* **2009**, *9*, 2125.
[45] C. Tasserit, A. Koutsioubas, D. Lairez, G. Zalczer, M. C. Clochard, *Phys. Rev. Lett.* **2010**, *105*, 1.
[46] J. Feng, K. Liu, R. D. Bulushev, S. Khlybov, D. Dumcenco, A. Kis, A. Radenovic, *Nat. Nanotechnol.* **2015**, *10*, 1070.
[47] K.-B. Jeong, K. Luo, M.-C. Lim, J.-Y. Jung, J.-S. Yu, K.-B. Kim, Y.-R. Kim, *Small* **2018**, *1801375*, 1801375.
[48] S. Marion, S. J. Davis, Z.-Q. Wu, A. Radenovic, *Nanoscale* **2020**, *12*, 8867.
[49] A. Naji, M. Kanducă, J. Forsman, R. Podgornik, *J. Chem. Phys.* **2013**, *139*, 150901.
[50] S. Garaj, W. Hubbard, a. Reina, J. Kong, D. Branton, J. a. Golovchenko, *Nature* **2010**, *467*, 190.
[51] K. Liu, J. Feng, A. Kis, A. Radenovic, *ACS Nano* **2014**, *8*, 2504.
[52] A. Marcotte, T. Mouterde, A. Nigués, A. Siria, L. Bocquet, *Nat. Mater.* **2020**, *19*, 1057.
[53] Z. Siwy, A. Fuliński, *Phys. Rev. Lett.* **2002**, *89*, 198103.
[54] M.-H. Hong, K. H. Kim, J. Bae, W. Jhe, *Appl. Phys. Lett.* **2000**, *77*, 2604.
[55] S. Manzeli, D. Ovchinnikov, D. Pasquier, O. V. Yazyev, A. Kis, *Nat. Rev. Mater.* **2017**, *2*, 17033.
[56] B. Rotenberg, O. Bernard, J.-P. Hansen, *J. Phys.: Conden. Matter.* **2018**, *30*, 054005.
[57] S. W. Coles, C. Park, R. Nikam, M. Kanducg, J. Dzubiella, B. Rotenberg, *J. Phys. Chem. B* **2020**, *124*, 1778, pMID: 32031810.
[58] R. Hartkamp, A.-L. Biance, L. Fu, J.-F. Dufrêche, O. Bonhomme, L. Joly, *Curr. Opin. Colloid Interface Sci.* **2018**, *37*, 101.
[59] S. Sahu, M. Zwolak, *Rev. Mod. Phys.* **2019**, *91*, 21004.
[60] R. Karnik, C. Duan, K. Castelino, H. Daiguji, A. Majumdar, *Nano Lett.* **2007**, *7*, 547.
[61] A. R. Poggioli, A. Siria, L. Bocquet, *J. Phys. Chem. B* **2019**, *123*, 1171.
[62] M. Špadina, S. Gourdin-Bertin, G. Dravzć, A. Selmani, J.-F. Dufrêche, K. Bohinc, *ACS Appl. Mater. Interfaces* **2018**, *10*, 13130, pMID: 29620855.
[63] C. Lee, L. Joly, A. Siria, A.-L. Biance, R. Fulcrand, L. Bocquet, *Nano Lett.* **2012**, *12*, 4037.
[64] N. Laohakunakorn, U. F. Keyser, *Nanotechnology* **2015**, *26*, 275202.
[65] M. Firnkes, D. Pedone, J. Knezevic, M. Doblinger, U. Rant, *Nano Lett.* **2010**, *10*, 2162.
[66] Y. Qiu, Z. S. Siwy, M. Wanunu, *Anal. Chem.* **2019**, *91*, 996.
[67] D. J. Rankin, L. Bocquet, D. M. Huang, *J. Chem. Phys.* **2019**, *151*, 044705.
[68] I. W. Leong, M. Tsutsui, S. Murayama, T. Hayashida, Y. He, M. Taniguchi, *ACS Appl. Mater. Interfaces* **2020**, *12*, 52175.
[69] H. Zhao, *J. Chem. Technol. Biotechnol.* **2015**, *90*, 19.
[70] S. K. Shukla, J.-P. Mikkola, *Front. Chem.* **2020**, *8*, 1219.
[71] A. Garai, D. Ghoshdastidar, S. Senapati, P. K. Maiti, *J. Chem. Phys.* **2018**, *149*, 045104.
[72] D. K. Sahoo, S. Jena, J. Dutta, S. Chakrabarty, H. S. Biswal, *ACS Central Sci.* **2018**, *4*, 1642.
[73] K. Jumbri, M. B. Abdul Rahman, E. Abdulmalek, H. Ahmad, N. M. Micaelo, *Phys. Chem. Chem. Phys.* **2014**, *16*, 14036.
[74] R. S. Dias, J. Innerlohinger, O. Glatter, M. G. Miguel, B. Lindman, *J. Phys. Chem. B* **2005**, *109*, 10458, pMID: 16852267.
[75] R. Austin, *Nat. Mater.* **2003**, *2*, 567.
[76] Y.-L. Wang, B. Li, S. Sarman, F. Mocci, Z.-Y. Lu, J. Yuan, A. Laaksonen, M. D. Fayer, *Chem. Rev.* **2020**, *120*, 5798, pMID: 32292036.
[77] M. Klahn, C. Stüber, A. Seduraman, P. Wu, *J. Phys. Chem. B* **2010**, *114*, 2856, pMID: 20146539.
[78] H. E. Bailey, Y.-L. Wang, M. D. Fayer, *J. Chem. Phys.* **2018**, *149*, 044501.
[79] B. L. Bhargava, Y. Yasaka, M. L. Klein, *Chem. Commun.* **2011**, *47*, 6228.
[80] A. Fang, K. Kroenlein, D. Riccardi, A. Smolyanitsky, *Nat. Mater.* **2019**, *18*, 76.
[81] E. Scoppola, E. B. Watkins, R. A. Campbell, O. Konovalov, L. Girard, J. F. Dufrêche, G. Ferru, G. Fragneto, O. Diat, *Angew. Chem. Int. Ed.* **2016**, *55*, 9326.
[82] Z. Liang, W. Bu, K. J. Schweighofer, D. J. Walwark, J. S. Harvey, G. R. Hanlon, D. Amoanu, C. Erol, I. Benjamin, M. L. Schlossman, *Proc. Natl. Ac. Sci.* **2019**, *116*, 18227.
[83] O. Nordness, J. F. Brennecke, *Chem. Rev.* **2020**, *120*, 12873, pMID: 33026798.
[84] H. V. Spohr, G. N. Patey, *J. Chem. Phys.* **2010**, *132*, 23 234510.
[85] M. Duvail, T. Dumas, A. Paquet, A. Coste, L. Berthon, P. Guilbaud, *Phys. Chem. Chem. Phys.* **2019**, *21*, 7894.
[86] M. Špadina, K. Bohinc, *Curr. Opin. Colloid Interface Sci.* **2020**, *46*, 94.
[87] O. Borodin, L. Suo, M. Gobet, X. Ren, F. Wang, A. Faraone, J. Peng, M. Olguin, M. Schroeder, M. S. Ding, E. Gobrogge, A. von Wald Cresce, S. Munoz, J. A. Dura, S. Greenbaum, C. Wang, K. Xu, *ACS Nano* **2017**, *11*, 10462, pMID: 29016112.
[88] Z. Liang, W. Bu, K. J. Schweighofer, D. J. Walwark, J. S. Harvey, G. R. Hanlon, D. Amoanu, C. Erol, I. Benjamin, M. L. Schlossman, *Proc. Natl. Acad. Sci.* **2019**, *116*, 18227.
[89] P.-M. Gassin, R. Champory, G. Martin-Gassin, J.-F. Dufrêche, O. Diat, *Colloids Surfaces A: Physicochem. Eng. Aspects* **2013**, *436*, 1103.
[90] T. Mo, S. Bi, Y. Zhang, V. Presser, X. Wang, Y. Gogotsi, G. Feng, *ACS Nano* **2020**, *14*, 2395, pMID: 31999427.
[91] K. Dong, X. Liu, H. Dong, X. Zhang, S. Zhang, *Chem. Rev.* **2017**, *117*, 6636, pMID: 28488441.
[92] A. Baer, Z. Miličević, D. M. Smith, A.-S. Smith, *J. Mol. Liquids* **2019**, *282*, 303.
[93] R. Futamura, T. Iiyama, Y. Takasaki, Y. Gogotsi, M. J. Biggs, M. Salanne, J. Ségalini, P. Simon, K. Kaneko, *Nat. Mater.* **2017**, *16*, 1225.
[94] F. Borghi, A. Podesta, *Adv. Phys.: X* **2020**, *5*, 1736949.
[95] A. M. Smith, A. A. Lee, S. Perkin, *J. Phys. Chem. Lett.* **2016**, *7*, 2157.
[96] V. Adibnia, M. Mirbagheri, P.-L. Latreille, G. De Crescenzo, D. Rochefort, X. Banquy, *Langmuir* **2019**, acs.langmuir.9b02011.
[97] R. Lhermerout, S. Perkin, *Phys. Rev. Fluids* **2018**, *3*, 014201.
[98] J. Comtet, A. Niguès, V. Kaiser, B. Coasne, L. Bocquet, A. Siria, *Nat. Mater.* **2017**, *16*, 634.
[99] R. S. Anaredy, S. K. Shaw, *Langmuir* **2016**, *32*, 5147.
[100] K. Ma, R. Jarosova, G. M. Swain, G. J. Blanchard, *Langmuir* **2016**, *32*, 9507.
[101] D. Pontoni, J. Haddad, B. M. Murphy, S. Festersen, O. Konovalov, B. M. Ocko, M. Deutsch, *J. Phys. Chem. C* **2019**, *123*, 3058.
[102] K. Shimizu, A. Pensado, P. Malfreyt, A. A. H. Padua, J. N. Canongia Lopes, *Faraday Discuss.* **2012**, *154*, 155.
[103] A. C. F. Mendonça, P. Malfreyt, A. A. H. Pädua, *J. Chem. Theory Comput.* **2012**, *8*, 3348, pMID: 26605741.
[104] M. Galluzzi, S. Bovio, P. Milani, A. Podestč, *J. Phys. Chem. C* **2018**, *122*, 14 7934.

[105] C. Merlet, B. Rotenberg, P. A. Madden, M. Salanne, *Phys. Chem. Chem. Phys.* **2013**, *15*, 15781.
[106] V. Kamysbayev, V. Srivastava, N. B. Ludwig, O. J. Borkiewicz, H. Zhang, J. Ilavsky, B. Lee, K. W. Chapman, S. Vaikuntanathan, D. V. Talapin, *ACS Nano* **2019**, *13*, 5760.
[107] M. Mezger, H. Schröder, H. Reichert, S. Schramm, J. S. Okasinski, S. Schöder, V. Honkimäki, M. Deutsch, B. M. Ocko, J. Ralston, M. Rohwerder, M. Stratmann, H. Dosch, *Science* **2008**, *322*, 424.
[108] Z. Brkljaca, M. Klimczak, Z. Milicevicä, M. Weisser, N. Taccardi, P. Wasserscheid, D. M. Smith, A. Magerl, A.-S. Smith, *J. Phys. Chem. Lett.* **2015**, *6*, 549, pMID: 26261977.
[109] L. Garcia, L. Jacquot, E. Charlaix, B. Cross, *Faraday Discuss.* **2018**, *206*, 443.
[110] S. Ntim, M. Sulpizi, *Phys. Chem. Chem. Phys.* **2020**, *22*, 19 10786.
[111] N. Vučemilović-Alagić, R. D. Banhatti, R. Stepic, C. R. Wick, D. Berger, M. U. Gaimann, A. Baer, J. Harting, D. M. Smith, A.-S. Smith, *Data in Brief* **2020**, *28*, 104794.
[112] N. Vučemilović-Alagić, R. D. Banhatti, R. Stepic, C. R. Wick, D. Berger, M. U. Gaimann, A. Baer, J. Harting, D. M. Smith, A.-S. Smith, *J. Colloid Interface Sci.* **2019**, *553*, 350.
[113] M. Salanne, *Phys. Chem. Chem. Phys.* **2015**, *17*, 14270.
[114] J. M. Otero-Mato, H. Montes-Campos, O. Cabeza, L. J. Gallego, L. M. Varela, *J. Mol. Liquids* **2020**, *320*, 114446.
[115] R. Singh Payal, S. Balasubramanian, *ChemPhysChem* **2012**, *13*, 1764.
[116] J.-M. Andanson, A. Baiker, *J. Phys. Chem. C* **2013**, *117*, 23 12210.
[117] M. Sobota, I. Nikiforidis, W. Hieringer, N. Paape, M. Happel, H.-P. Steinrück, A. Görling, P. Wasserscheid, M. Laurin, J. Libuda, *Langmuir* **2010**, *26*, 7199, pMID: 20143797.
[118] K. C. Jha, H. Liu, M. R. Bockstaller, H. Heinz, *J. Phys. Chem. C* **2013**, *117*, 49 25969.
[119] E. S. C. Ferreira, C. M. Pereira, M. N. D. S. Cordeiro, D. J. V. A. dos Santos, *J. Phys. Chem. B* **2015**, *119*, 9883, pMID: 26101957.
[120] J. J. Segura, A. Elbourne, E. J. Wanless, G. G. Warr, K. Voïtchovsky, R. Atkin, *Phys. Chem. Chem. Phys.* **2013**, *15*, 3320.
[121] R. Atkin, S. Z. El Abedin, R. Hayes, L. H. S. Gasparotto, N. Borisenko, F. Endres, *J. Phys. Chem. C* **2009**, *113*, 30 13266.
[122] Y. Zuo, Y. Zhang, R. Huang, Y. Min, *Phys. Chem. Chem. Phys.* **2019**, *21*, 22.
[123] M. M. Huang, Y. Jiang, P. Sasisanker, G. W. Driver, H. Weingärtner, *J. Chem. Eng. Data* **2011**, *56*, 1494.
[124] M. A. Gebbie, M. Valtiner, X. Banquy, E. T. Fox, W. A. Henderson, J. N. Israelachvili, *Proc. Natl. Acad. Sci. U. S. A.* **2013**, *110*, 24 9674.
[125] M. A. Gebbie, H. A. Dobbs, M. Valtiner, J. N. Israelachvili, *Proc. Natl. Acad. Sci.* **2015**, *112*, 7432.
[126] A. A. Lee, C. S. Perez-Martinez, A. M. Smith, S. Perkin, *Phys. Rev. Lett.* **2017**, *119*, 026002.
[127] J. C. Araque, J. J. Hettige, C. J. Margulis, *J. Phys. Chem. B* **2015**, *119*, 12727.
[128] G. Feng, M. Chen, S. Bi, Z. A. Goodwin, E. B. Postnikov, N. Brilliantov, M. Urbakh, A. A. Kornyshev, *Phys. Rev. X* **2019**, *9*, 021024.
[129] H. Tokuda, K. Hayamizu, K. Ishii, M. A. B. H. Susan, M. Watanabe, *J. Phys. Chem. B* **2005**, *109*, 6103, pMID: 16851672.
[130] S. Tsuzuki, W. Shinoda, H. Saito, M. Mikami, H. Tokuda, M. Watanabe, *J. Phys. Chem. B* **2009**, *113*, 10641, pMID: 19591511.
[131] M. E. Di Pietro, F. Castiglione, A. Mele, *J. Mol. Liquids* **2020**, *322*, 114567.
[132] L. Daukiya, J. Seibel, S. D. Feyter, *Adv. Phys.: X* **2019**, *4*, 1625723.
[133] A. Balan, C. C. Chien, R. Engelke, M. Drndic, *Sci. Rep.* **2015**, *5*, September 1.
[134] L. J. de Vreede, C. Ying, J. Houghtaling, J. Figueiredo Da Silva, A. R. Hall, A. Lovera, M. Mayer, *Nanotechnology* **2019**, *30*, 265301.
[135] M. Graf, M. Lihter, M. Thakur, V. Georgiou, J. Topolancik, B. R. Ilic, K. Liu, J. Feng, Y. Astier, A. Radenovic, *Nat. Protoc.* **2019**, *14*, 1130.
[136] K. R. Seddon, A. Stark, M.-J. Torres, *Pure Appl. Chem.* **2000**, *72*, 2275.
[137] G. Ori, C. Massobrio, A. Pradel, M. Ribes, B. Coasne, *Langmuir* **2015**, *31*, 6742, pMID: 26030830.
[138] S. Park, J. G. McDaniel, *J. Chem. Phys.* **2020**, *152*, 7 074709.
[139] E. H. Lahrar, A. Belhboub, P. Simon, C. Merlet, *ACS Appl. Mater. Interfaces* **2020**, *12*, 1789, pMID: 31805764.
[140] W. V. Karunaratne, C. J. Margulis, *J. Phys. Chem. C* **2019**, *123*, 34 20971.
[141] A. Einstein, in *Investigations on the Theory of the Brownian Movement*, Dover Books on Physics Series, Dover Publications, New York **1956**.
[142] R. Kubo, *J. Phys. Soc. Japan* **1957**, *12*, 570.
[143] Y. He, R. Qiao, J. Vatamanu, O. Borodin, D. Bedrov, J. Huang, B. G. Sumpter, *J. Phys. Chem. Lett.* **2016**, *7*, 36, pMID: 26641287.
[144] B. Coasne, L. Viau, A. Vioux, *J. Phys. Chem. Lett.* **2011**, *2*, 1150, pMID: 26295318.
[145] I. C. Bourg, G. Sposito, *J. Colloid Interface Sci.* **2011**, *360*, 701
[146] G. Feng, X. Jiang, R. Qiao, A. A. Kornyshev, *ACS Nano* **2014**, *8*, 11685, pMID: 25341189.
[147] B. Docampo-Álvarez, V. Gómez-González, H. Montes-Campos, J. M. Otero-Mato, T. Méndez-Morales, O. Cabeza, L. J. Gallego, R. M. Lynden-Bell, V. B. Ivaništšev, M. V. Fedorov, L. M. Varela, *J. Phys.: Conden. Matter* **2016**, *28*, 464001.
[148] T. Kobayashi, A. Kemna, M. Fyta, B. Braunschweig, J. Smiatek, *J. Phys. Chem. C* **2019**, *123*, 13795.
[149] A. M. Smith, A. A. Lee, S. Perkin, *J. Phys. Chem. Lett.* **2016**, *7*, 2157, pMID: 27216986.
[150] J. Zeman, S. Kondrat, C. Holm, *Chem. Commun.* **2020**, *56*, 15635.
[151] N. Dubouis, C. Park, M. Deschamps, S. Abdelghani-Idrissi, M. Kanduč, A. Colin, M. Salanne, J. Dzubiella, A. Grimaud, B. Rotenberg, *ACS Central Sci.* **2019**, *5*, 640.
[152] S. Maset, K. Bohinc, *J. Phys. A: Math. Theor.* **2007**, *40*, 11815.
[153] H. Zhang, M. Zhu, W. Zhao, S. Li, G. Feng, *Green Energy Environ.* **2018**, *3*, 120.
[154] V. A. Parsegian, *Van der Waals Forces: A Handbook for Biologists, Chemists, Engineers, and Physicists*, Cambridge University Press, Cambridge, UK **2005**.
[155] R. H. French, V. A. Parsegian, R. Podgornik, R. F. Rajter, A. Jagota, J. Luo, D. Asthagiri, M. K. Chaudhury, Y.-m. Chiang, S. Granick, S. Kalinin, M. Kardar, R. Kjellander, D. C. Langreth, J. Lewis, S. Lustig, D. Wesolowski, J. S. Wettlaufer, W.-Y. Ching, M. Finnis, F. Houlihan, O. A. von Lilienfeld, C. J. van Oss, T. Zemb, *Rev. Mod. Phys.* **2010**, *82*, 1887.
[156] J. P. Thiruraman, P. Masih Das, M. Drndić, *ACS Nano* **2020**, *14*, 3736, pMID: 32195580.
[157] S. Bi, R. Wang, S. Liu, J. Yan, B. Mao, A. Kornyshev, G. Feng, *Nat. Commun.* **2018**, *9*, 5222.
[158] D. Ghoshdastidar, S. Senapati, *Soft Matter* **2016**, *12*, 3032.
[159] E. L. Ratkova, D. S. Palmer, M. V. Fedorov, *Chem. Rev.* **2015**, *115*, 6312, pMID: 26073187.
[160] D. Ben-Yaakov, D. Andelman, R. Podgornik, D. Harries, *Curr. Opin. Colloid Interface Sci.* **2011**, *16*, 542.
[161] D. H. Mengistu, K. Bohinc, S. May, *Europhys. Lett.* **2009**, *88*, 14003.
[162] A. Igličg, E. Gongadze, K. Bohinc, *Bioelectrochemistry* **2010**, *79*, 223.
[163] Y. A. Budkov, A. L. Kolesnikov, Z. A. Goodwin, M. G. Kiselev, A. A. Kornyshev, *Electrochim. Acta* **2018**, *284*, 346.
[164] M. McEldrew, Z. A. H. Goodwin, A. A. Kornyshev, M. Z. Bazant, *J. Phys. Chem. Lett.* **2018**, *9*, 5840, pMID: 30229648.
[165] G. Allaire, J.-F. Dufrêche, A. Mikelić, A. Piatnitski, *Nonlinearity* **2013**, *26*, 881.

[166] C. Merlet, M. Salanne, B. Rotenberg, P. A. Madden, *Electrochim. Acta* **2013**, *101*, 262.
[167] K. Pivnic, F. Bresme, A. A. Kornyshev, M. Urbakh, *ACS Appl. Nano Mater.* **2020**, *3*, 10708.
[168] Y. Zhang, P. T. Cummings, *ACS Appl. Mater. Interfaces* **2019**, *11*, 42680, pMID: 31608619.
[169] T. Méndez-Morales, J. Carrete, O. Cabeza, L. J. Gallego, L. M. Varela, *J. Phys. Chem. B* **2011**, *115*, 11170, pMID: 21899260.
[170] Z. Lu, S. Dourdain, S. Pellet-Rostaing, *Langmuir* **2020**, *36*, 12121, pMID: 32845649.
[171] M. Špadina, K. Bohinc, T. Zemb, J.-F. Dufrêche, *ACS Nano* **2019**, *13*, 13745.
[172] M. Z. Bazant, M. S. Kilic, B. D. Storey, A. Ajdari, *Adv. Colloid Interface Sci.* **2009**, *152*, 48.
[173] S. Kondrat, P. Wu, R. Qiao, A. A. Kornyshev, *Nat. Mater.* **2014**, *13*, 387.
[174] A. A. Lee, S. Kondrat, D. Vella, A. Goriely, *Phys. Rev. Lett.* **2015**, *115*, 106101.
[175] A. Schlaich, E. W. Knapp, R. R. Netz, *Phys. Rev. Lett.* **2016**, *117*, 048001.
[176] Y. Lauw, M. D. Horne, T. Rodopoulos, F. A. M. Leermakers, *Phys. Rev. Lett.* **2009**, *103*, 117801.
[177] J. Forsman, C. E. Woodward, M. Trulsson, *J. Phys. Chem. B* **2011**, *115*, 4606, pMID: 21456566.
[178] A. L. Kiratidis, S. J. Miklavcic, *J. Chem. Phys.* **2019**, *150*, 18 184502.
[179] A. A. Lee, D. Vella, S. Perkin, A. Goriely, *J. Phys. Chem. Lett.* **2015**, *6*, 159, pMID: 26263105.
[180] A. Smolyanitsky, E. Paulechka, K. Kroenlein, *ACS Nano* **2018**, *12*, 6677.
[181] S. Sahu, J. Elenewski, C. Rohmann, M. Zwolak, *Sci. Adv.* **2019**, *5*, 7 eaaw5478.
[182] B. L. Bhargava, M. L. Klein, *Soft Matter* **2009**, *5*, 3475.
[183] Y. Matsubara, D. C. Grills, Y. Koide, *ACS Omega* **2016**, *1*, 1393.
[184] F. Capuani, I. Pagonabarraga, D. Frenkel, *J. Chem. Phys.* **2004**, *121*, 2 973.
[185] B. Rotenberg, I. Pagonabarraga, D. Frenkel, *Faraday Discuss.* **2010**, *144*, 223.
[186] N. Rivas, S. Frijters, I. Pagonabarraga, J. Harting, *J. Chem. Phys.* **2018**, *148*, 14 144101.
[187] N. Dubouis, A. Serva, R. Berthin, G. Jeanmairet, B. Porcheron, *J. Chem. Phys.* **2019**, *151*, 11 114104.
[188] N. Kulyk, D. Berger, A.-S. Smith, J. Harting, *Comp. Phys. Commun.* **2020**, *256*, 107443.
[189] K. N. Marsh, J. A. Boxall, R. Lichtenthaler, *Fluid Phase Equilib.* **2004**, *219*, 93.
[190] M. Taha, F. A. E Silva, M. V. Quental, S. P. Ventura, M. G. Freire, J. A. Coutinho, *Green Chem.* **2014**, *16*, 3149.
[191] A. Benedetto, P. Ballone, *ACS Sustain. Chem. Eng.* **2016**, *4*, 392.
[192] C. Zhu, M. Varona, J. L. Anderson, *ACS Omega* **2020**, *5*, 11151.
[193] J. Sweeney, F. Hausen, R. Hayes, G. B. Webber, F. Endres, M. W. Rutland, R. Bennewitz, R. Atkin, *Phys. Rev. Lett.* **2012**, *109*, 155502.
[194] O. Y. Fajardo, F. Bresme, A. A. Kornyshev, M. Urbakh, *Sci. Rep.* **2015**, *5*, 7698.
[195] M. Puster, J. A. Rodríguez-Manzo, A. Balan, M. Drndić, *ACS Nano* **2013**, *7*, 11283, pMID: 24224888.
[196] S. J. Heerema, L. Vicarelli, S. Pud, R. N. Schouten, H. W. Zandbergen, C. Dekker, *ACS Nano* **2018**, *12*, 2623.
[197] S.-W. Nam, M. J. Rooks, K.-B. Kim, S. M. Rossnagel, *Nano Lett.* **2009**, *9*, 2044.
[198] Z. Jiang, D. Stein, *Phys. Rev. E - Stat. Nonlinear, Soft Matter Phys.* **2011**, *83*, 1.
[199] S. J. Davis, M. Macha, A. Chernev, D. M. Huang, A. Radenovic, S. Marion, *Nano Lett.* **2020**, *20*, 8089.